Structure, Directional-Correlation, and Doppler-Shift Lifetime Measurements in ^{61}Cu via ^{58}Ni(^{4}He, $p\gamma$) Reaction Spectrometry

D. G. Sarantites, J. H. Barker, and N.-H. Lu
Department of Chemistry, Washington University, St. Louis, Missouri 63130*

E. J. Hoffman and D. M. Van Patter
Bartol Research Foundation of the Franklin Institute,† Swarthmore, Pennsylvania 19081

(Received 12 March 1973)

The level structure and the decay properties of the levels in ^{61}Cu up to 4082 keV of excitation have been carefully investigated via prompt $\gamma\gamma$ and $p\gamma$ coincidence experiments employing Ge(Li) γ-ray detectors and annular Si surface-barrier charged-particle detectors. From these experiments and from high-resolution singles energy and directional-correlation measurements an improved decay scheme has been obtained which includes 44 levels in ^{61}Cu and incorporates 120 γ rays. New levels at 2584.5, 3739.4, 3942.4, and 4081.8 keV were postulated, while the γ decay of several previously reported levels between 3277–3802 keV was not observed. The singles directional correlations from many transitions were used to obtain (i) reliable branching ratios for the more intense γ rays and (ii) multipole mixing ratios $\delta(E2/M1)$ by employing both a ratio method and an independent analysis of the correlations via the compound statistical theory of nuclear reactions. Branching ratios for the weaker γ rays were obtained from spectra taken at 55° to the beam direction. The lifetimes of 31 levels in ^{61}Cu were measured by the Doppler-shift attenuation method via the ^{58}Ni(^{4}He, $p\gamma$) reaction at bombardment energies between 9.7 and 12.2 MeV. Lifetimes were extracted from singles spectra obtained at 0, 15, 30, 45, 70, 90, and 110° and from $p\gamma$ coincidence spectra obtained at 0° to the beam direction, by employing both a centroid shift analysis for the data from all angles and a line-shape fitting analysis for the data from angles $\leq 45°$. The stopping power of Ni previously calibrated for Cu ions, was used for the line-shape analysis and for obtaining reliable $F(\tau)$ curves applicable to the present conditions of both the singles and the coincidence experiments. For a large number of transitions in ^{61}Cu values for $B(E2)$ and $B(M1)$ were obtained. The $B(E2)$ and $B(M1)$ values together with the $\delta(E2/M1)$ values and the branching ratios from the first 10 levels in ^{61}Cu are compared with recent detailed calculations for ^{61}Cu based on a unified model. Good general agreement is observed between experiment and theory for the $B(E2)$ values. Only moderate agreement between experiment and theory is observed for the $B(M1)$ and $\delta(E2/M1)$ values.

I. INTRODUCTION

The low-lying levels of nuclei occupying the p-f shell in the vicinity of nickel have recently been the subject of extensive calculations. In particular the level structure and the electromagnetic properties for at least 10 levels in ^{59,61,63,65}Cu have recently been calculated by Castel, Johnstone, Singh, and Stewart.[1] These authors[1] have given an extensive summary of previous calculations of the properties of the odd-A Cu isotopes. The calculations of Castel *et al.*[1] are based on a unified model derived from the coupling of the $f_{7/2}, f_{5/2}, p_{3/2}$, and $p_{1/2}$ orbitals with the anharmonic vibrations of the core. The strength of the core-particle quadrupole interaction is the only adjustable parameter in the calculation[1] with the diagonal and off-diagonal matrix elements of the quadrupole interaction taken from the quadrupole moments and $B(E2)$ values for the core nickel nuclei. The effects of pairing interaction have also been included in the calculation of Castel *et al.*[1] Other calculations that reported $M1$ and transition rates are those of Larner[2] and Gomez.[3] Neither of these calculations, however, include anharmonic or quasiparticle effects. The results of Larner[2] and Gomez[3] have been compared[2,3] with limited-transition-rate data for ^{61,63,65}Cu, while the more complete calculations of Castel *et al.*[1] have been compared[1] with limited-rate data only for ^{63,65}Cu.

The level structure of ^{61}Cu has been studied in some detail recently both from the decay[4-6] of 89.1-sec ^{61}Zn and from in-beam ^{58}Ni(^{4}He, $p\gamma$) high-resolution spectrometry.[7,8] The present investigation was undertaken in order to obtain (a) a more detailed scheme for the level structure of ^{61}Cu and (b) accurate values of the transition rates [$B(E2)$ and $B(M1)$] for as many transitions as possible in ^{61}Cu. A more detailed scheme[8] for ^{61}Cu is essential in the evaluation of previous[9] and new[10] level yield data from studies of nuclear-reaction mechanisms currently under investigation. Furthermore, accurate values for $B(E2)$ and $B(M1)$ for many transitions in ^{61}Cu can provide a powerful test of the validity of model calculations such as those of Castel *et al.*[1] In this work we have been able to construct a detailed scheme for the decay of 44 levels in ^{61}Cu which incorporates 120 γ rays. New

levels at 2584.5, 3739.4, 3942.4, and 4081.8 keV have been postulated, while the decay of previously reported[8] levels at 3277, 3584, 3591, 3613, 3647, 3695, 3755, 3802, 3950, and 3988 keV was not observed in this work. The lifetimes of 31 states in ^{61}Cu have been measured via the Doppler-shift attenuation (DSA) method using the ^{58}Ni-(^{4}He, $p\gamma$) reaction. These results were obtained employing a stopping power for ^{61}Cu ions in ^{58}Ni which was previously calibrated[11] to give line shapes and lifetimes for some transitions in ^{63}Cu that have been measured via resonance fluorescence techniques. The lifetimes measured by Heusch, Cujec, and Dayras[12] are systematically lower than the present measurements. From this work, multipole mixing ratios $\delta(E2/M1)$ were obtained for many transitions from singles angular correlations. Values of $B(E2)$ and $B(M1)$ for many transitions in ^{61}Cu were obtained from the present lifetimes and from present and previous[7,8] multipole mixing ratios. The results for the transitions from the first 10 levels in ^{61}Cu are compared with the calculations of Castel *et al.*[1] and the agreement and deviations are discussed.

II. EXPERIMENTAL PROCEDURES

A. Accelerators and Scattering Chambers

The external beam facility[13] of the Washington University cyclotron provided the 10.0–20.0-MeV ^{4}He^{++} beams required. For energies below 12.2 MeV the beam energy was degraded by means of Au foils. All the coincidence experiments were performed above 12.2 MeV. Also, in many of the DSA measurements the tandem Van de Graaff accelerator of the University of Pennsylvania was used.

Several miniature scattering chambers were used in coincidence experiments which permitted the positioning of the annular Si particle detectors at a distance of 1.0–10.0 cm from the target and of the Ge(Li) γ detector at a distance of $\geq$2.5 cm for all angles between 0°–90° to the beam. Uniform Ta or Pb lining was employed inside the chambers in order to reduce the γ-ray background from the stopping beam. The collimators through the annular particle detectors were also made of Ta or Pb. In order to reduce the background from the back-scattered ^{4}He^{++} particles from the beam stop, Al absorbers with a hole slightly larger than the beam size were placed either at the target position or in front of the particle detector. In the latter case all the α particles scattered from the target were stopped in the absorber. For the coincidence experiments at 20 MeV a different small scattering chamber was used that permitted the beam to stop 3 m downstream from the detectors.

B. Detection Equiptment and Methods of Counting

The charged-particle detectors were 200-mm^2 $\times$1.0-mm annular Si surface-barrier detectors which were cooled either with a thermoelectric cooler or with a cold finger to −67°. This reduced the leakage current by a factor of $\simeq$100 and greatly improved detector stability. In these experiments the subtended angles were from 145°–170°. For neutron detection a 12.7-cm$\times$12.7-cm NE-213 liquid scintillator was employed. This detector was positioned at 4.0 cm from the target at 90° to the beam for the $n\gamma$ coincidence experiments. A detailed description of this system and the pulse-shape discrimination arrangement is given in Ref. 13.

Two Ge(Li) γ-ray detectors were employed (33 and 35 cm^3) which had actual resolutions of 4.0 and 2.2 keV full width at half maximum at 1332 keV measured at the end of each experiment. Calibration γ-ray peaks were introduced in the $p\gamma$ coincidence spectra by requiring coincidences between the Ge(Li) detector and a 5.08-cm$\times$5.08-cm NaI(Tl) detector, which was shielded from the target but viewed a ^{207}Bi source that was also visible to the Ge(Li) detector. For singles measurements the same scattering chambers were used and the Ge(Li) detectors were employed in anti-Compton arrangements which have been described in Refs. 14 and 15. These anti-Compton spectrometers and their shieldings were located on angular correlation tables that permitted spectra to be taken between 0 and 110° to the beam direction.

The targets were isotopically enriched to 99.95% in ^{58}Ni and consisted of 2.0- and 3.8-mg/cm^2 foils prepared by rolling of the metals. For some of the experiments 2 mg/cm^2 of Au were evaporated on the back side of the target in order to prevent the recoils from decaying in flight in the vacuum.

For data collection and partial data reduction a 4096-channel pulse-height analyzer was used which was interfaced to a PDP 8/L computer that had a buffer tape with 24-bit related address capability.

C. Extraction of Lifetimes

Mean lifetimes were determined for many transitions in ^{61}Cu via the DSA method from γ-ray spectra obtained from singles measurements between 0°–110° and from $p\gamma$ coincidence measurements at 0° to the beam. The lifetimes were extracted from comparison with experiment using both a line-shape fitting technique and the $F(\tau)$ or centroid-shift technique, which have been described in considerable detail in Ref. 11, where an evaluation of the effect of the various parameters of the DSA method was also given. Briefly, it can be shown[11]

that the energy shift of a γ ray emitted at an angle θ_d to the beam direction from an ensemble of nuclei moving with velocity $v(t)/c=\beta(\theta_R, t)$ is given by

$$\Delta E_\gamma = E_\gamma^0 \beta(\theta_R, t)\cos\theta_c(t) \times(\cos\theta_R\cos\theta_d+\sin\theta_R\sin\theta_d\sin\phi_R), \quad (1)$$

where the polar angles θ_R, ϕ_R define the direction of the recoils at $t=0$ and $\cos\theta_c(t)$ is the average collision cosine as given by Blaugrund.[16] The fraction of reactions that lead to decay via the state of interest between t and $t+dt$ and give an energy shift ΔE_γ is

$$\frac{dN(\Delta E_\gamma)}{N^0} = R(t)dt\frac{d\sigma(\theta_R)}{d\Omega}d\Omega d\phi W(\theta_R\phi_R\theta_d), \quad (2)$$

where $R(t)$ is the fraction of nuclei that decay per unit time through the state of interest at time t: $d\sigma(\theta_R)/d\Omega$ is the relative differential cross section for the initial emission of recoils at an angle θ_R, and $W(\theta_R\phi_R\theta_d)$ is the angular correlation function for the emission of a γ ray at an angle θ_d to the beam when the initial recoil was emitted in the direction defined by θ_R, ϕ_R. The line spectrum is obtained via Eqs. (1) and (2) by allowing t, θ_R, and ϕ_R to take their possible values.[11] Expressions for evaluating $d\sigma(\theta_R)/d\Omega$ and $W(\theta_R\phi_R\theta_d)$ to a reasonable approximation have been given in Ref. 11.

The centroid shift is given by

$$\langle\Delta E_\gamma\rangle = \overline{E}_\gamma - E_\gamma^0 = E_\gamma^0\overline{\beta}(0)F(\tau)\cos\theta_d, \quad (3)$$

where

$$F(\tau)=\frac{1}{\overline{\beta}(0)}\int_0^\infty R(t)\cos\theta_c(t)\overline{\beta}(t)dt$$

with

$$\overline{\beta}(t)=\int_{\theta_R} d\Omega\frac{d\sigma(\theta_R)}{d\Omega}W(\theta_R\theta_d)\beta(\theta_R t)\cos\theta_R .$$

The quantity $F(\tau)$ is the ratio of the observed shift and the shift that would be observed if all decays occurred at time zero.

In order to evaluate $\beta(\theta_R, t)$ the stopping power theory of Lindhard, Scharff, and Schiott[17] (LSS) as modified by Blaugrund[16] was employed with the

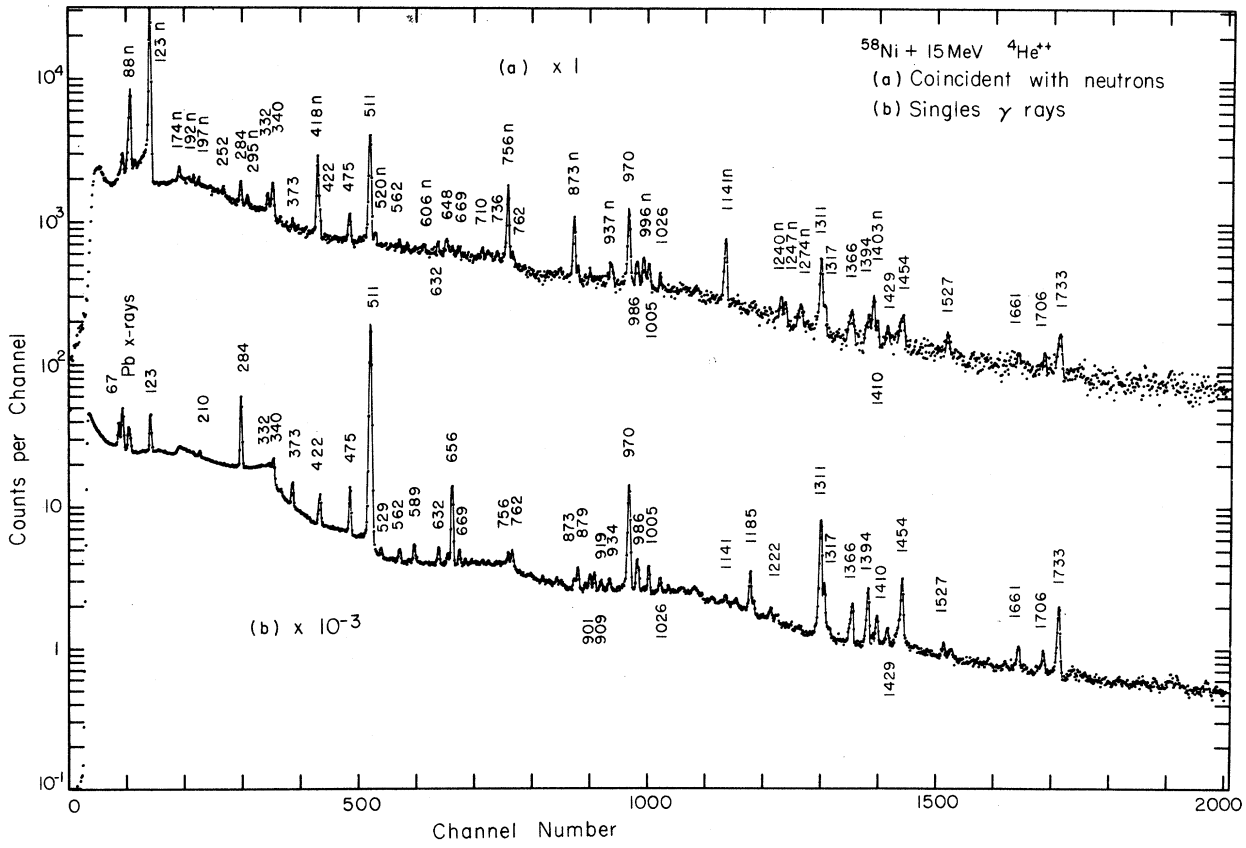

FIG. 1. (a) Spectrum of the γ rays coincident with neutron pulses subsequent to $^4He^{++}$ bombardment of ^{58}Ni at 15.0 MeV. (b) Singles spectrum of the γ rays taken with the same gain for a short time for the purpose of comparison.

stopping power taken as

$$\frac{d\epsilon}{d\rho}=f_e\left(\frac{d\epsilon}{d\rho}\right)_e+f_n\left(\frac{d\epsilon}{d\rho}\right)_n,$$

where $(d\epsilon/d\rho)_e=k\epsilon^{1/2}$ and $(d\epsilon/d\rho)_n=\epsilon^{1/2}/(0.67+2.07\epsilon+0.03\epsilon^2)$ are the electronic and nuclear stopping powers, respectively. The quantities ϵ and ρ are the LSS dimensionless parameters for energy and length. The factors f_e and f_n have been introduced to adjust the two stopping powers relative to the values of the LSS theory to fit the line shapes and lifetimes of "standard" γ rays with lifetimes measured by different techniques, such as resonance fluorescence. In this work the values of $f_e=f_n=0.84$ were employed which were obtained[11] for the stopping power of Ni for Cu ions. In the present analysis the effect of the recoils escaping the target (<10%) and decaying in vacuum on the calculated line shapes of the $F(\tau)$ was properly taken into account. Also, for some of the singles measurements the observed state was found to receive partial population from other higher-lying states. In these cases the feeding from higher states was properly taken into account when the line shapes or the $F(\tau)$ values were calculated.[11]

III. EXPERIMENTAL RESULTS

A. Energies and Branching Ratios of γ Rays from ^{58}Ni(^{4}He, $p\gamma$)^{61}Cu

The energies of the γ rays from the ^{58}Ni(^{4}He, $p\gamma$) reaction were measured at the bombardment energies of 10.0 and 12.2 MeV. They were determined from high-resolution singles spectra taken with the anti-Compton spectrometer at 90°. The energies of many new weak γ rays were determined utilizing as internal standards (i) the most intense γ rays in ^{61}Cu for which accurate values[5,6] exist from the decay of ^{61}Zn, and (ii) the γ rays from the decay[18] of ^{61}Cu. Spectra from 10.0-MeV bombardments did not include γ rays from the ^{58}Ni-(^{4}He, $n\gamma$) reaction (threshold 10.1 MeV) and populated states up to ~3200 keV with substantial yield. Many of the higher-lying high-spin states ($J\geq\frac{9}{2}$) receive substantial cross section at the 12.2-MeV bombardment energy. In order to determine the prompt γ rays associated with the (^{4}He, $n\gamma$) reaction an $n\gamma$-coincidence experiment was performed at 15.0 MeV of ^{4}He^{++} bombardment energy in which neutrons were detected with a 12.7-cm×12.7-cm NE-213 liquid scintillator and the γ rays with a Ge(Li) detector positioned at 55° to the beam direction. The γ-ray events were rejected from the neutron detector by pulse-shape discrimination as described in Ref. 13. In Fig. 1(a) the γ-ray spectrum coincident with neutrons is shown. The random events have not been subtracted. For purposes of comparison Fig. 1(b) shows a singles γ-ray spectrum taken with the same gain for a short time. Peaks in true coincidence with neutrons are labeled by n and correspond to the energies of 88, 123, 174, 192, 197, 295, 418, 520, 606, 756, 873, 937, 996, 1141, 1240, 1247, 1274, and 1403 keV.

A high-resolution Compton-suppressed singles spectrum of the γ rays from the ^{4}He^{++} bombardment of ^{58}Ni at 12.2 MeV taken at 90° to the beam is shown in Fig. 2. This spectrum shows many of the γ peaks from Ref. 8 resolved into doublets and includes a considerable number of new weak γ rays. The γ-ray energies determined in this work are summarized in column 5 of Table I. Columns 1 and 2 in Table I give the level No. and level energy established in this work as a weighted average of the sums of γ-ray energies leading to each level. Levels below 3259.6 keV have been well established previously.[8] Arguments for new levels and new assignments of γ rays are given below in Sec. IV. Columns 3 and 4 give the J^π values and the transition numbers as established in this work (Sec. IV).

The branching ratios of the γ rays deexciting each proposed level are summarized in column 6 of Table I. These were determined from measurements of singles angular distributions of γ rays relative to the beam direction. These experiments were performed at 10.0-MeV ^{4}He^{++} bombardment energy so that ^{61}Zn was not produced. The branching ratios for many of the γ rays from levels with $J\geq\frac{7}{2}$ were also obtained from the 12.2-MeV data, since these levels are not observed[4-6] in the decay of ^{61}Zn. Additional measurements for the branching ratios were obtained from singles spectra taken at 55° to the beam direction. At this angle $P_2(\cos\theta)$ vanishes and reasonable values for the branching ratios are obtained provided $A_4\ll 1$ [see Eq. (4) below]. For some low-spin levels which are only weakly populated in the (^{4}He, $p\gamma$) reaction the branching ratios from Refs. 5 and 6 have been adopted as indicated in Table I.

B. $\gamma\gamma$ Coincidence Experiments

Although the $p\gamma$-coincidence experiments from Ref. 8 and from this work gave conclusive evidence for many level and γ-ray assignments, a $\gamma\gamma$-coincidence experiment with two Ge(Li) detectors at higher bombardment energy was considered essential and it provided the coincidence relationships between γ rays deexciting the states that are believed to be of high spin. The results of such an experiment at 20-MeV ^{4}He^{++} energy are summarized in Table II. The first column gives the level(s) from which the γ ray(s) in the gate originate.

The second column gives the γ rays in the digital gate and the last column the γ rays observed in the coincidence spectra.

C. Angular Correlation Measurements

The angular correlations of most γ rays from ^{61}Cu following the ^{58}Ni(^{4}He, $p\gamma$) reaction at 10.0 MeV were determined in singles experiments. These correlations were obtained using as a monitor the intensity of the 475.0-keV γ ray which was shown[8] to be isotropic. The singles correlations obtained were analyzed by a least-squares fit of the data to the function

$$W(\theta) = A_0[1 + A_2 Q_2 P_2(\cos\theta) + A_4 Q_4 P_4(\cos\theta)], \tag{4}$$

where Q_k are the attenuation factors due to the finite solid angle of the Ge(Li) detector.[19,20] The A_0 values obtained give the branching ratios reported in Table I. In the present analysis the formalism and phase conventions of Rose and Brink[21] were employed. Thus the A_k terms of Eq. (4) above are given by

$$A_k(J_1 J_2 \delta) = B_k(J_1)\ \frac{R_k(LLJ_1J_2) + 2\delta R_k(LL'J_1J_2) + \delta^2 R_k(L'L'J_1J_2)}{(1+\delta^2)} \tag{5}$$

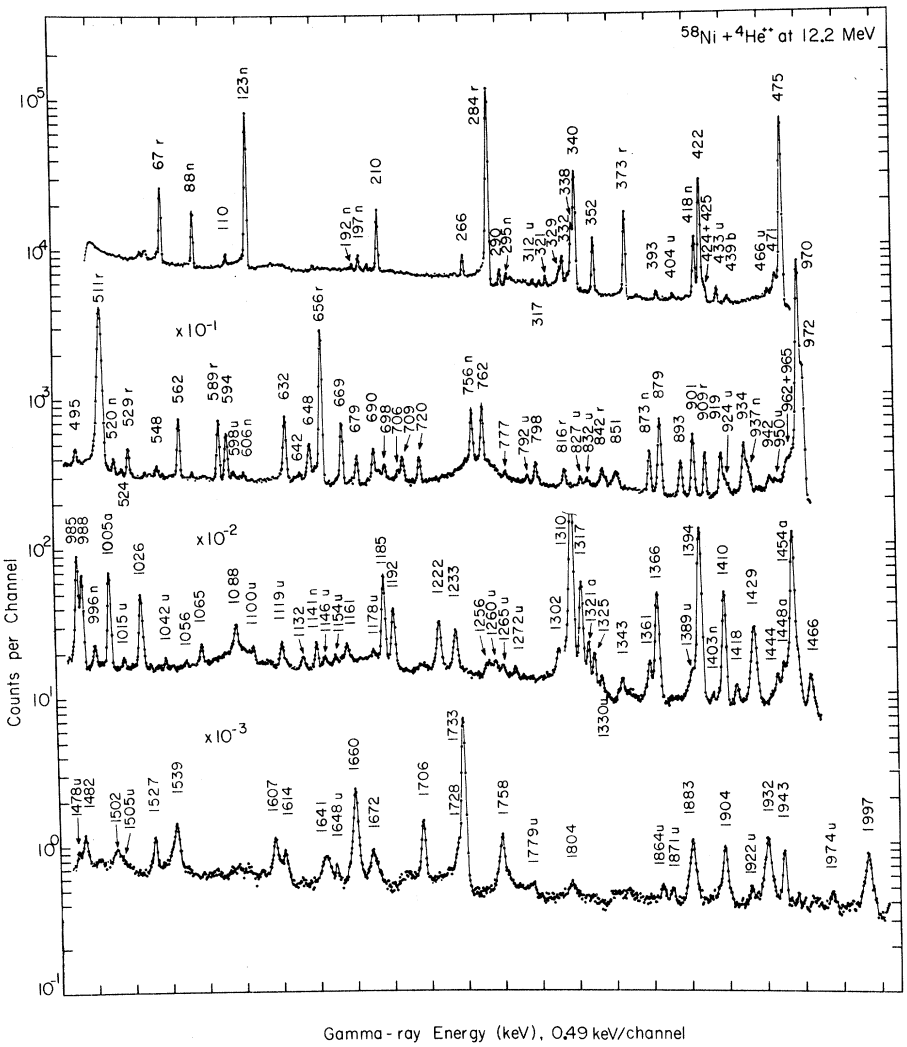

FIG. 2. High-resolution Compton-suppressed singles spectrum of the γ rays from the ^{58}Ni(^{4}He, $p\gamma$)^{61}Cu reaction at 12.2 MeV taken at 90° to the beam direction. Peaks associated with γ rays from the ^{58}Ni(^{4}He, $n\gamma$)^{61}Zn reaction are labeled n and those unassigned are labeled u. Peaks associated with the ^{58}Ni(^{4}He, $\alpha'\gamma$) reaction are labeled a and those from ^{61}Cu decay are labeled r. Some Doppler broadening is apparent for some of the high-energy peaks.

TABLE I. Summary of level energies, J^π values, γ-ray energies, and γ-ray branching ratios for transitions in ^{61}Cu determined in this work.

Level No.	Level energy (keV)	J^π	Transition	γ-ray energy (keV)	Branching (%)
0	0	$\frac{3}{2}^-$			
1	475.0 ± 0.1	$\frac{1}{2}^-$	1→0	475.0 ± 0.1	100
2	970.0 ± 0.1	$\frac{5}{2}^-$	2→1	494.8 ± 0.2	0.9 ± 0.1
			2→0	970.0 ± 0.1	99.1 ± 0.6
3	1310.4 ± 0.2	$\frac{7}{2}^-$	3→2	340.2 ± 0.3	6.2 ± 0.2
			3→0	1310.5 ± 0.2	93.8 ± 0.2
4	1394.1 ± 0.2	$\frac{5}{2}^-$	4→2	424.1 ± 0.3	2.8 ± 0.3
			4→1	919.1 ± 0.2	11.9 ± 0.6
			4→0	1394.2 ± 0.2	85.3 ± 2.5
5	1660.24 ± 0.11	$\frac{3}{2}^-$	5→4	265.9 ± 0.2	4.6 ± 0.3
			5→2	690.2 ± 0.2	15.7 ± 1.2
			5→1	1185.3 ± 0.3	14.4 ± 0.9
			5→0	1660.5 ± 0.2	65.3 ± 1.5
6	1732.51 ± 0.15	$\frac{7}{2}^-$	6→4	338.4 ± 0.3	2.3 ± 0.5
			6→3	421.8 ± 0.2	22.4 ± 3.4
			6→2	762.4 ± 0.2	13.6 ± 1.0
			6→0	1732.7 ± 0.2	61.8 ± 3.0
7	1904.1 ± 0.2	$\frac{5}{2}^-$	7→3	593.5 ± 0.2	22.1 ± 1.0
			7→2	934.1 ± 0.2	41.6 ± 1.3
			7→0	1904.2 ± 0.3	36.3 ± 1.9
8	1932.6 ± 0.2	$\frac{3}{2}^-$	8→2	962.4 ± 0.5	7.6 ± 1.1
			8→1	1457.8 ± 0.2	25.3 ± 1.7
			8→0	1932.4 ± 0.3	67.1 ± 4.3
9	1942.35 ± 0.15	$\frac{7}{2}^-$	9→6	209.6 ± 0.2	9.9 ± 0.2
			9→4	548.0 ± 0.3	0.5 ± 0.1
			9→3	631.9 ± 0.2	19.2 ± 0.5
			9→2	972.4 ± 0.4	60 ± 4
			9→0	1942.8 ± 0.3	10.4 ± 0.6
10	2088.7 ± 0.2	$\frac{1}{2}^-$	10→1	1613.7 ± 0.2	32 ± 3 [a]
			10→0	2088.7 ± 0.3	68 ± 7 [a]
11	2203.25 ± 0.16	$\frac{5}{2}^-$	11→6	470.8 ± 0.2	11.4 ± 0.8
			11→3	892.8 ± 0.2	18.7 ± 0.6
			11→2	1233.3 ± 0.2	46.8 ± 0.6
			11→1	1728.2 ± 0.3	23.1 ± 1.4
12	2295.0 ± 0.2	$\frac{9}{2}^-$	12→9	352.4 ± 0.2	7.6 ± 0.4
			12→6	562.4 ± 0.2	19.9 ± 0.6
			12→4	900.8 ± 0.2	25.8 ± 0.8
			12→3	984.6 ± 0.2	34.2 ± 1.1

TABLE I *(Continued)*

Level No.	Level energy (keV)	J^π	Transition	γ-ray energy (keV)	Branching (%)
			12→2	1325.3±0.3	12.5±0.7
13	2336.2±0.2	$\frac{9}{2}^-$	13→9	393.4±0.4	1.7±0.7
			13→4	942.2±0.5	1.2±0.2
			13→3	1025.8±0.3	22.0±1.3
			13→2	1366.4±0.3	75.1±2.2
14	2358.1±0.2	$(\frac{1}{2}-\frac{5}{2})^-$	14→8	425.3±0.3	11.1±0.6 [a]
			14→5	697.6±0.3	30.7±2.7 [a]
			14→1	1883.1±0.3	34.6±0.7 [a]
			14→0	2358.6±0.3	23.6±1.7 [a]
15	2398.9±0.3	$\frac{7}{2}^-$	15→3	1088.4±0.3	41.8±1.0
			15→2	1429.0±0.3	58.2±2.8
16	2472.3±0.2	$\frac{3}{2}^-$	16→2	1502.4±0.3	10.7±1.2
			16→1	1997.3±0.3	89.3±2.4
17	2583.6±0.3	$(\frac{7}{2}, \frac{9}{2})^-$	17→9	641.5±0.3	18±3
			17→6	850.9±0.3	82±9
18	2584.5±0.5	$(\frac{3}{2}, \frac{5}{2})^-$	18→0	2584.5±0.5	100
19	2611.8±0.2	$\frac{9}{2}^-$	19→12	316.6±0.2	1.4±0.1
			19→9	669.3±0.2	30.1±0.5
			19→6	879.3±0.2	58.6±1.7
			19→3	1301.7±0.3	9.9±0.7
20	2626.8±0.2	$\frac{11}{2}^-$	20→13	290.4±0.2	1.6±0.1
			20→12	331.6±0.4	2.6±0.3
			20→3	1316.7±0.2	95.8±3.1
21	2684.0±0.3	$\frac{3}{2}^-$	21→4	1289.8±0.6	≤2.7
			21→1	2209.0±0.2	53.3±3.0
			21→0	2683.8±0.8	42.9±3.0
22	2720.2±0.3	$\frac{9}{2}^+$	22→19	109.5±0.2	4.6±0.7
			22→15	320.9±0.2	1.2±0.3
			22→9	777.2±0.3	1.4±0.4
			22→6	987.6±0.3	37.7±5.0
			22→3	1409.9±0.2	55.1±1.8
23	2728.0±0.2	$\frac{7}{2}^-$	23→15	328.8±0.4	2.7±0.3
			23→11	524.5±0.3	3.9±0.4 [b]
			23→3	1417.8±0.2	33.2±1.6
			23→2	1758.2±0.3	60.2±7.5
24	2792.5±0.3	$\frac{5}{2}^-$	24→3	1482.2±0.3	51±4
			24→0	2792.4±0.3	49±5
25	2840.6±0.3	$(\frac{1}{2})^-$	25→10	751.6±0.2	56±6 [a]
			25→0	2841.5±0.6	44±4 [a]

TABLE I *(Continued)*

Level No.	Level energy (keV)	J^{π}	Transition	γ-ray energy (keV)	Branching (%)
26	2857.0 ± 0.4	$(\frac{1}{2}-\frac{5}{2})^-$	26→1	2381.4 ± 2.0	20 ± 3
			26→0	2857.0 ± 0.3	80 ± 12
27	2923.9 ± 0.3	$(\frac{9}{2})^-$	27→20	297.4 ± 0.2	4.4 ± 0.6
			27→19	312.0 ± 0.2	2.4 ± 0.6
			27→15	524.5 ± 0.2	4.4 ± 0.6 [b]
			27→12	629.1 ± 0.5	2.6 ± 0.6
			27→9	981.3 ± 0.5	9.3 ± 1.8
			27→6	1191.8 ± 0.4	77.0 ± 4.4
28	2932.5 ± 0.4	$\frac{3}{2}^-$	28→4	1538.9 ± 0.2	10 ± 1 [a]
			28→1	2457.6 ± 0.4	78 ± 5 [a]
			28→0	2931.8 ± 0.4	12 ± 3 [a]
29	3001.5 ± 0.3	$(\frac{7}{2}^-,\frac{3}{2}^-)$	29→11	789.0 ± 0.3	13.5 ± 0.9
			29→4	1607.3 ± 0.2	26.2 ± 2.0
			29→0	3002.6 ± 0.5	60.3 ± 3.2
30	3015.6 ± 0.2	$\frac{11}{2}^-$	30→13	679.2 ± 0.2	13.7 ± 1.4
			30→12	720.5 ± 0.2	13.4 ± 1.3
			30→3	1705.4 ± 0.3	72.9 ± 3.6
31	3019.2 ± 1.4	$\frac{3}{2}^-$	31→1	2543.9 ± 3.0	71 ± 13
			31→0	3019.3 ± 1.1	29 ± 4
32	3065.5 ± 0.5	$(\frac{3}{2},\frac{5}{2})^-$	32→14	706.4 ± 0.5	9.8 ± 0.9
			32→7	1161.1 ± 0.3	39.2 ± 3.1
			32→4	1672.1 ± 0.4	30.8 ± 2.8
			32→0	3065.9 ± 0.5	20.2 ± 3.0
33	3092.0 ± 0.5	$(\frac{3}{2},\frac{5}{2})^-$	33→0	3092.0 ± 0.5	100
34	3198.4 ± 0.3		34→9	1256.0 ± 0.4	26 ± 6
			34→6	1466.1 ± 0.3	46 ± 7
			34→4	1804.1 ± 0.5	28 ± 9
35	3259.6 ± 0.3	$(\frac{11}{2})^-$	35→19	647.9 ± 0.3	39.7 ± 1.3
			35→12	964.8 ± 0.5	13.3 ± 1.8
			35→6	1527.4 ± 0.5	47.0 ± 4.1
36	3322.9 ± 0.5		36→3	2012.5 ± 0.5	100
37	3373.3 ± 0.5	$(\frac{9}{2}^-)$	37→6	1640.6 ± 0.5	100
38	3454.4 ± 0.3		38→15	1055.8 ± 0.5	5.1 ± 0.3
			38→6	1721.7 ± 0.5	20 ± 6
			38→3	2143.9 ± 0.5	75 ± 12
39	3521.1 ± 1.5	$(\frac{1}{2}-\frac{5}{2})^-$	39→0	3521.1 ± 1.5	100
40	3546.6 ± 0.4		40→11	1343.4 ± 0.3	100
41	3739.4 ± 0.5	$(\frac{11}{2}^-)$	41→12	1444.4 ± 0.4	100
42	3852.6 ± 0.5	$(\frac{5}{2}-\frac{9}{2})^+$	42→22	1132.4 ± 0.4	100

TABLE I *(Continued)*

Level No.	Level energy (keV)	J^π	Transition	γ-ray energy (keV)	Branching (%)
43	3942.4 ± 0.5	$(\frac{7}{2}-\frac{11}{2})^+$	43→22	1222.2 ± 0.3	100
44	4081.8 ± 0.5	$(\frac{7}{2}-\frac{11}{2})^+$	44→37	709.6 ± 0.4	24.6 ± 4.7
			44→22	1361.3 ± 0.3	75.4 ± 3.8

[a] Average value from Refs. 5 and 6.
[b] Assigned by energy fit to deexcite more than one level.

with

$$B_k(J_1) = \sum_{M_1=1/2}^{J_1} p(M_1)\rho_k(J_1 M_1) \tag{5'a}$$

which is applicable for the two lowest multipoles L and $L' = L+1$ contributing to the γ-ray transition between $J_1 \to J_2$. The statistical tensors $\rho_k(J_1 M_1)$ have been defined by Rose and Brink.[21] In this work multipole mixing ratios $\delta(E2/M1)$ were obtained for those transitions for which another known branch from the same level of pure $E2$ character was also observed. By this ratio method, using Eq. (5) and assuming a pure $E2$ transition $J_1 \to J_3$ one obtains

$$\frac{A_k(J_1 J_2 \delta)}{A_k(J_1 J_3 E2)} = \frac{R_k(LLJ_1J_2) + 2\delta R_k(LL'J_1J_2) + \delta^2 R_k(L'L'J_1J_2)}{R_k(22J_1J_3)(1+\delta^2)} . \tag{6}$$

The values of δ from the ratio method were obtained by solving the quadratic equation (6) for $k = 2$. The results are summarized in column 4 of Table III. In this table the first column gives the transition, the second column gives the transition energy in keV, the third column gives the angular momentum sequence $J_i^\pi \to J_f^\pi$ as deduced in this work, and columns 6 and 7 summarize the δ

TABLE II. Summary of the $\gamma\gamma$ coincidence relationships established in this work in 20-MeV $^4He^{++}$ bombardment of ^{58}Ni and from decay of ^{61}Zn of Ref. 5.

E_{level} (keV)	E_γ (keV) in the gate	E_γ (keV) observed in coincidence
475	475 [a]	1185, 1458, 1614, 1883, 1997, 2209, 2458
970	970 [a]	690, 934
970, 1942	970, 972	340, 352, 422, 669, 690, 708 [b], 762, 851, 934, 970, 972, 1026, 1366, 1429
1310	1310 [a]	1482
1310	1310	422, 632, 669 [b], 799, 985, 1026, 1317, 1361, 1410, 1526, 1705
1394	1394	338, 901
1733	422	340, 562, 851, 879, 988, 1310, 1361
1733	1733	210, 352 [b], 562, 851, 879, 988, 1361, 1527
1904	934	970
2295	562	338 + 340, 422, 721, 762, 1733
2336	1366	970
2612	669	210, 632, 648, 972, 1311
2612	879	422, 648, 762, 1733
2628	1317	340, 970 [b], 1310
2721	1410	340, 1132, 1222, 1310, 1361
3016	1705	340, 1310
3260	1527	422, 762, 1733
4082	1361	422, 970 [b], 987, 1310, 1410

[a] Coincidences observed (see Ref. 9) in the decay of ^{61}Zn.
[b] Observed in weak coincidence.

TABLE III. Summary of the multipole mixing ratios determined in this work.

Transition	Transition energy (keV)	$J^\pi_i \rightarrow J^\pi_f$	$\delta(E2/M1)$ ratio method	$\delta(E2/M1)$ CN theory [a]	$\delta(E2/M1)$ Hoffman *et al.* (Ref. 8)	$\delta(E2/M1)$ Heusch *et al.* (Ref. 7)	$\delta(E2/M1)$ adopted
1→0	475.0	$\frac{1}{2}^- \rightarrow \frac{3}{2}^-$					0.04 [b]
2→0	970.0	$\frac{5}{2}^- \rightarrow \frac{3}{2}^-$			0.30 ± 0.04	0.38 ± 0.03	0.35 ± 0.03
2→1	494.8	$\frac{5}{2}^- \rightarrow \frac{1}{2}^-$					$E2$
3→1	1310.5	$\frac{7}{2}^- \rightarrow \frac{3}{2}^-$	$(E2)$			$-(0.01 \pm 0.03)$ [c]	$E2$
3→2	340.2	$\frac{7}{2}^- \rightarrow \frac{5}{2}^-$	0.027 ± 0.023		0.01 ± 0.02	$0.00^{+0.09}_{-0.07}$	0.016 ± 0.012
4→1	919.1	$\frac{5}{2}^- \rightarrow \frac{1}{2}^-$	$(E2)$		$E2$	$-(0.03^{+0.08}_{-0.12})$ [c]	$E2$
4→0	1394.1	$\frac{5}{2}^- \rightarrow \frac{3}{2}^-$	$2.99^{+0.71}_{-0.56}$		2.9 ± 0.4	3.64 ± 0.14	3.54 ± 0.13
5→2	690.2	$\frac{3}{2}^- \rightarrow \frac{5}{2}^-$			$-(0.30 \pm 0.14)$ or ≥ 4.9	$0.10^{+0.11}_{-0.09}$ or $3.10^{+1.40}_{-0.90}$	$-(0.04 \pm 0.16)$ or $3.1^{+1.4}_{-0.9}$
5→1	1185.3	$\frac{3}{2}^- \rightarrow \frac{1}{2}^-$				$0.26 \leq \delta \leq 1.00$	$0.26 \leq \delta \leq 1.00$
5→0	1660.2	$\frac{3}{2}^- \rightarrow \frac{3}{2}^-$			$-1.56 \leq \delta \leq -0.33$	$-(1.37^{+0.28}_{-0.35})$ or $-(0.39^{+0.18}_{-0.10})$	$-(1.37^{+0.23}_{-0.35})$ or $-(0.39^{+0.18}_{-0.10})$
6→4	338.4	$\frac{7}{2}^- \rightarrow \frac{5}{2}^-$	$1.2^{+0.5}_{-0.9}$				$1.2^{+0.5}_{-0.9}$
6→3	421.8	$\frac{7}{2}^- \rightarrow \frac{7}{2}^-$	$-(0.11 \pm 0.03)$		$-(0.24^{+0.10}_{-0.15})$	$0.20^{+0.09}_{-0.07}$ or $-(1.20 \pm 0.27)$	$-(0.080 \pm 0.043)$
6→2	762.4	$\frac{7}{2}^- \rightarrow \frac{5}{2}^-$	$-(0.52 \pm 0.04)$		$-(0.45 \pm 0.08)$	$-(0.37^{+0.13}_{-0.10})$	$-(0.50 \pm 0.03)$
6→0	1732.5	$\frac{7}{2}^- \rightarrow \frac{3}{2}^-$	$(E2)$			$0.02^{+0.06}_{-0.04}$ [c]	$E2$
7→3	593.5	$\frac{5}{2}^- \rightarrow \frac{3}{2}^-$		$0.091^{+0.023}_{-0.026}$	0.05 ± 0.03	$0.15^{+0.15}_{-0.13}$	$0.076^{+0.020}_{-0.022}$
7→2	934.1	$\frac{5}{2}^- \rightarrow \frac{5}{2}^-$		$0.20^{+0.05}_{-0.04}$	0.14 ± 0.04	$0.06^{+0.10}_{-0.15}$	0.18 ± 0.03
7→0	1904.1	$\frac{5}{2}^- \rightarrow \frac{3}{2}^-$		$-(0.68^{+0.09}_{-0.07})$		$-(0.78^{+0.50}_{-0.12})$	$-(0.69^{+0.09}_{-0.06})$
8→1	1457.8	$\frac{3}{2}^- \rightarrow \frac{1}{2}^-$				$-(0.20^{+0.07}_{-0.10})$ or 3.0 ± 0.8	$-(0.20^{+0.07}_{-0.10})$ or 3.0 ± 0.8
8→0	1932.6	$\frac{3}{2}^- \rightarrow \frac{3}{2}^-$		$-(0.26^{+0.12}_{-0.08})$ or $-(1.82^{+0.54}_{-0.29})$		$-0.42 \leq \delta \leq 0.08$ or $-2.48 \leq \delta \leq 1.19$	$-(0.26^{+0.12}_{-0.08})$ or $-(1.82^{+0.54}_{-0.29})$
9→6	209.6	$\frac{7}{2}^- \rightarrow \frac{7}{2}^-$	0.14 ± 0.05	$0.01^{+0.03}_{-0.04}$	$-(0.15 \pm 0.08)$		0.030 ± 0.052

TABLE III *(Continued)*

Transition	Transition energy (keV)	$J^\pi_i \to J^\pi_f$	$\delta(E2/M1)$ ratio method	$\delta(E2/M1)$ CN theory [a]	$\delta(E2/M1)$ Hoffman *et al.* (Ref. 8)	$\delta(E2/M1)$ Heusch *et al.* (Ref. 7)	$\delta(E2/M1)$ adopted
9→3	631.9	$\frac{7}{2}^- \to \frac{7}{2}^-$		$0.08^{+0.14}_{-0.12}$	0.26 ± 0.06 or $-(0.76 \pm 0.16)$	$0.51 \le \delta \le 1.54$ or $-0.70 \le \delta \le 0.05$	0.23 ± 0.07
9→0	1942.4	$\frac{7}{2}^- \to \frac{3}{2}^-$	$(E2)$	$(0.08^{+0.15}_{-0.12})$ [c]			$E2$
11→3	892.8	$\frac{5}{2}^- \to \frac{7}{2}^-$		0.01 ± 0.03 or $9.2^{+2.2}_{-1.8}$			0.01 ± 0.03 or $9.2^{+2.2}_{-1.8}$
11→2	1233.3	$\frac{5}{2}^- \to \frac{5}{2}^-$		$0.030^{+0.022}_{-0.035}$			$0.030^{+0.022}_{-0.035}$
11→1	1728.2	$\frac{5}{2}^- \to \frac{1}{2}^-$					$E2$
12→9	352.4	$\frac{9}{2}^- \to \frac{7}{2}^-$	$0.24^{+0.10}_{-0.08}$	0.11 ± 0.04	0.35 ± 0.05		0.20 ± 0.08
12→6	562.4	$\frac{9}{2}^- \to \frac{7}{2}^-$	$-(1.2 \pm 0.5)$	$-(0.56 \pm 0.04)$	$-(0.56 \pm 0.10)$		$-(0.56 \pm 0.04)$
12→4	900.8	$\frac{9}{2}^- \to \frac{5}{2}^-$	$(E2)$	0.026 ± 0.062 [c]			$E2$
12→3	984.6	$\frac{9}{2}^- \to \frac{7}{2}^-$		$0.19^{+0.04}_{-0.03}$	0.13 ± 0.05		$0.170^{+0.031}_{-0.026}$
12→2	1325.3	$\frac{9}{2}^- \to \frac{5}{2}^-$					$E2$
13→4	942.2	$\frac{9}{2}^- \to \frac{5}{2}^-$					$E2$
13→3	1025.8	$\frac{9}{2}^- \to \frac{7}{2}^-$	0.20 ± 0.03	0.38 ± 0.05			0.25 ± 0.08
13→2	1366.4	$\frac{9}{2}^- \to \frac{5}{2}^-$	$(E2)$	0.022 ± 0.024 [c]			$E2$
15→3	1088.4	$\frac{7}{2}^- \to \frac{7}{2}^-$		$-(0.60^{+0.22}_{-0.41})$			$-(0.60^{+0.22}_{-0.41})$
15→2	1429.0	$\frac{7}{2}^- \to \frac{5}{2}^-$		$+0.164 \pm 0.024$	$0.82 \le \delta \le 1.7$		0.164 ± 0.024
16→1	1997.3	$\frac{13}{2}^- \to \frac{1}{2}^-$		$+0.017 \pm 0.045$ or 0.87 ± 0.09			0.017 ± 0.045 or 0.87 ± 0.09
19→9	669.3	$\frac{9}{2}^- \to \frac{7}{2}^-$		$-(0.25^{+0.05}_{-0.03})$			$-(0.25^{+0.05}_{-0.03})$
19→6	879.3	$\frac{9}{2}^- \to \frac{7}{2}^-$		$-(0.33 \pm 0.02)$	$-(0.64 \pm 0.06)$		$-(0.36 \pm 0.10)$
20→3	1316.7	$\frac{11}{2}^- \to \frac{7}{2}^-$	$(E2)$	$-(0.066 \pm 0.066)$ [c]			$E2$
22→6	987.6	$\frac{9}{2}^+ \to \frac{7}{2}^-$		0.00 ± 0.03 [d]			$E1$
22→3	1409.9	$\frac{9}{2}^+ \to \frac{7}{2}^-$		0.035 ± 0.030 [d]	0.18 ± 0.05		$E1$
23→3	1417.8	$\frac{7}{2}^- \to \frac{7}{2}^-$		$-(0.36^{+0.67}_{-0.42})$			$-(0.36^{+0.67}_{-0.42})$

TABLE III (*Continued*)

Transition	Transition energy (keV)	$J^\pi_i \rightarrow J^\pi_f$	$\delta(E2/M1)$ ratio method	$\delta(E2/M1)$ CN theory[a]	$\delta(E2/M1)$ Hoffman *et al.* (Ref. 8)	$\delta(E2/M1)$ Heusch *et al.* (Ref. 7)	$\delta(E2/M1)$ adopted
23→2	1758.2	$\frac{7}{2}^- \rightarrow \frac{5}{2}^-$		$1.55^{+0.34}_{-0.30}$			$1.55^{+0.34}_{-0.30}$
27→6	1191.8	$\frac{9}{2}^- \rightarrow \frac{7}{2}^-$		0.00 ± 0.05			0.00 ± 0.05
30→12	720.5	$\frac{11}{2}^- \rightarrow \frac{9}{2}^-$	$-(0.02 \pm 0.06)$	0.01 ± 0.02			0.01 ± 0.02
30→3	1705.4	$\frac{11}{2}^- \rightarrow \frac{7}{2}^-$	(*E*2)	$-(0.035 \pm 0.060)$[c]			*E*2
31→1	2543.9	$\frac{3}{2}^- \rightarrow \frac{1}{2}^-$		$0.58^{+0.34}_{-0.26}$			$0.58^{+0.34}_{-0.26}$

[a] Values obtained from singles angular correlations analyzed with the aid of the computer code MANDY based on the statistical model for nuclear reactions for the prediction of the γ-ray angular distributions. The quoted uncertainties refer to a 95% confidence limit and were estimated as suggested in Ref. 27.
[b] Theoretical value given by Castel *et al.* (Ref. 1).
[c] Multipole mixing ratio for *M*3/*E*2.
[d] Multipole mixing ratio for *M*2/*E*1.

values from Refs. 8 and 7, respectively.

Additional values for the multipole mixing ratios δ were extracted from the singles correlation measurements for transitions from levels not involving $E2$ branches by applying the Hauser-Feshbach theory of nuclear reactions[22] to a theoretical analysis of the singles γ-ray distributions. For this purpose a program called MANDY originally written by Sheldon and Strang[23] employing the formalism of Sheldon and Van Patter[24] was modified to compute the $B_k(J_1)$ factors of Eq. (5). The proton transmission coefficients were taken from the compilation of Mani, Melkanoff, and Iori[25] and the α-particle transmission coefficients were calculated with an optical-model code using the best-fit

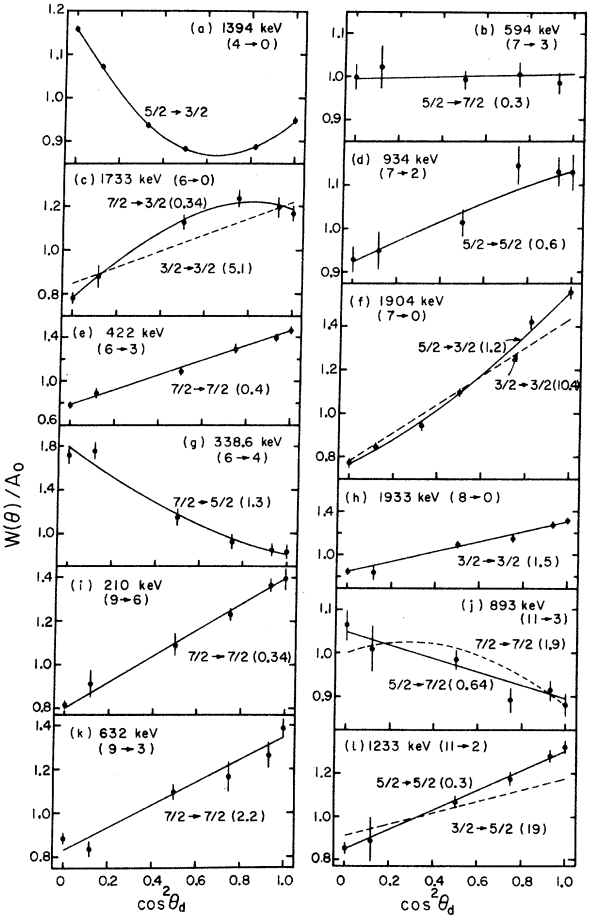

FIG. 3. Singles angular distributions of the γ rays indicated in keV for the transition identified by the integers in parentheses. The quantity $W(\theta_d)/A_0$ is plotted vs $\cos^2\theta_d$. The solid curves are the theoretical correlations for the δ value that gave the minimum χ^2 value indicated in parentheses after the spin sequence. The dashed or dotted curves show the correlations for alternate spin sequences obtained for δ values giving the minimum χ^2 values shown in parentheses. These sequences have been rejected as unlikely.

parameters for ^{58}Ni of Fulmer, Benveniste, and Mitchell.[26] The theoretical correlations obtained in this way with the $A_k(J_1J_2\delta)$ terms of Eq. (5) were fitted to the data and a χ^2 value was computed as function of δ. The J^π values for many levels in ^{61}Cu were uniquely determined primarily due to the fact that for all cases examined, correlations for at least two transitions from each level were obtained experimentally, so that alternate J^π assignments could be eliminated from at least one or more correlations. The results are summarized in the fifth column of Table III. Here we point out that the 900.8-, 1366.4-, 1316.7-, and 1705.4-keV transitions are expected (see Sec. IV) to be pure $E2$ transitions. The $\delta(M3/E2)$ values given in column 5 of Table III for these transitions are zero within experimental error for all of these. Furthermore, the 987.6- and 1409.9-keV transitions are expected (see Sec IV) to be pure $E1$ in character and this is confirmed by the very small $\delta(M2/E1)$ ratios obtained as shown in column 5 of Table III. These consistency checks clearly show that the compound-nucleus theory[22-24] employed here correctly reproduces the nuclear spin alignment for this reaction. Reliable values, therefore, for $\delta(E2/M1)$ should be obtained as indicated in column 5 in Table III for the transitions in ^{61}Cu for which no previous measurements are available. The quoted uncertainties for the δ values correspond to a 95% confidence limit and were evaluated as described by Cline and Lesser.[27] We should further point out that for some of the correlations analyzed a small fraction of decay ($\leq$18%) from higher-lying levels was observed. In these cases the $B_k(J_1)$ values were obtained by the proper corrections with the $U_k(J'J_1\delta')$ linking parameters for

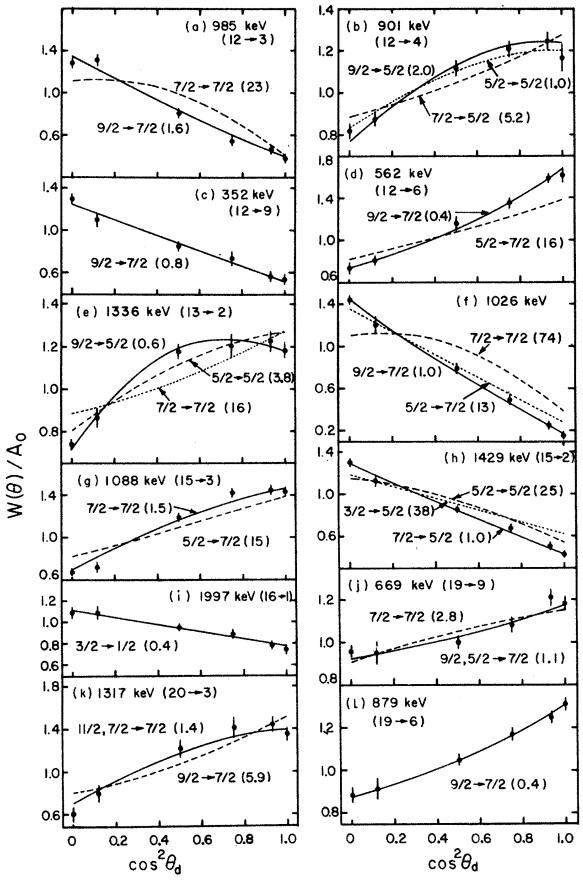

FIG. 4. Singles angular distributions of the γ rays indicated in keV for the transition identified by the integers in parentheses. The quantity $W(\theta_d)/A_0$ is plotted vs $\cos^2\theta_d$. The solid curves are the theoretical correlations for the δ value that gave the minimum χ^2 value in parentheses after the spin sequence. The dashed or dotted curves show the correlations for alternate spin sequences obtained for δ values giving the minimum χ^2 values shown in parentheses. These sequences have been rejected as unlikely.

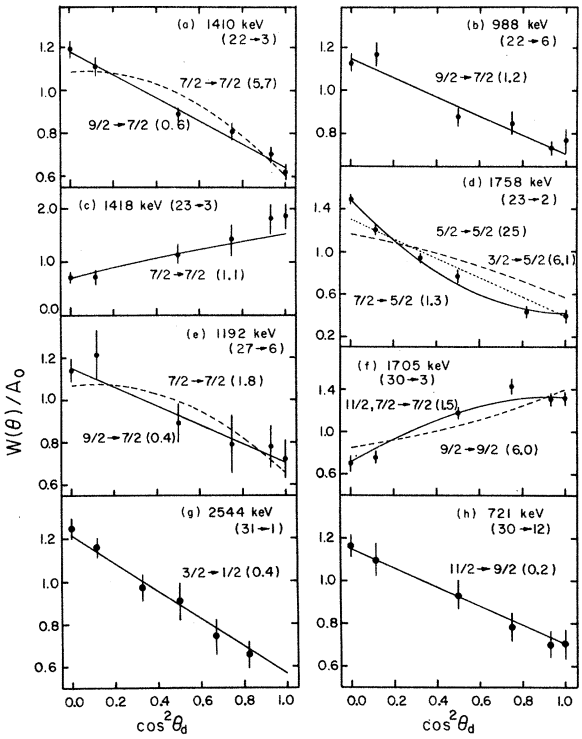

FIG. 5. Singles angular distributions of the γ rays indicated in keV for the transition identified by the integers in parentheses. The quantity $W(\theta_d)/A_0$ is plotted vs $\cos^2\theta_d$. The solid curves are the theoretical correlations for the δ value that gave the minimum χ^2 value indicated in parentheses after the spin sequence. The dashed or dotted curves show the correlations for alternate spin sequences obtained for δ values giving the minimum χ^2 values shown in parentheses. These sequences have been rejected as unlikely.

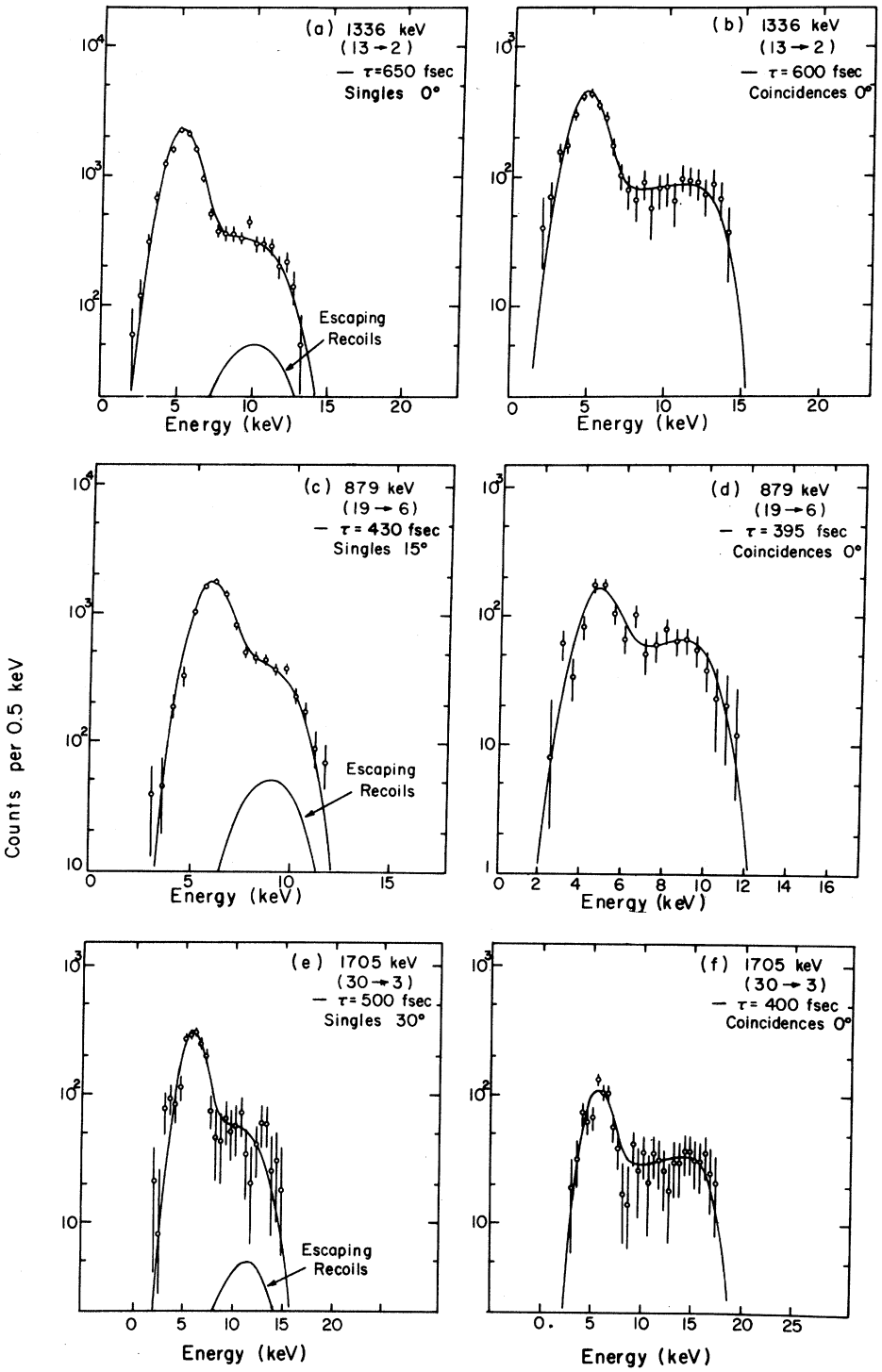

FIG. 6. Comparison with the data of the theoretical line shapes used to obtain lifetimes for the 1336.4-, 879.3-, and 1705.4-keV γ rays from singles spectra at the indicated angles and from coincidence data at 0°. The spectrum of the escaping recoils is shown for the singles data. The coincidence data were obtained with a target with Au backing so that the recoils excaping the Ni were stopped in Au. The theoretical lines shown for all cases correspond to those that gave the minimum χ^2 value.

the unobserved transitions as tabulated by Rose and Brink.[21] For some of these unobserved transitions the mixing ratios δ' are not known. For these cases calculations with δ' taken as 0 or 0.3 showed that the $B_k(J_1)$ values differed by no more than 1–2% and such an additional uncertainty was incorporated in the analysis. The last column of Table III summarizes the adopted values for $\delta(E2/M1)$ which were obtained from columns 4–7 as weighted averages using weights based on the quoted uncertainties.

In Figs. 3, 4, and 5 we show the singles correlations that were obtained, plotted as a function of $\cos^2\theta_d$. These correlations provide evidence for many new definite J^π assignments and confirm many previous assignments in ^{61}Cu. The solid curves in Figs. 3–5 are the theoretical correlations for the accepted spin sequences which gave the J^π and δ values shown in Table III and correspond to the minimum values of χ^2 shown in parentheses after each spin sequence in the figures. The integer numbers in parentheses in Figs. 3–5, after the transition energy given in keV, help identify the transition. The dashed or dotted curves

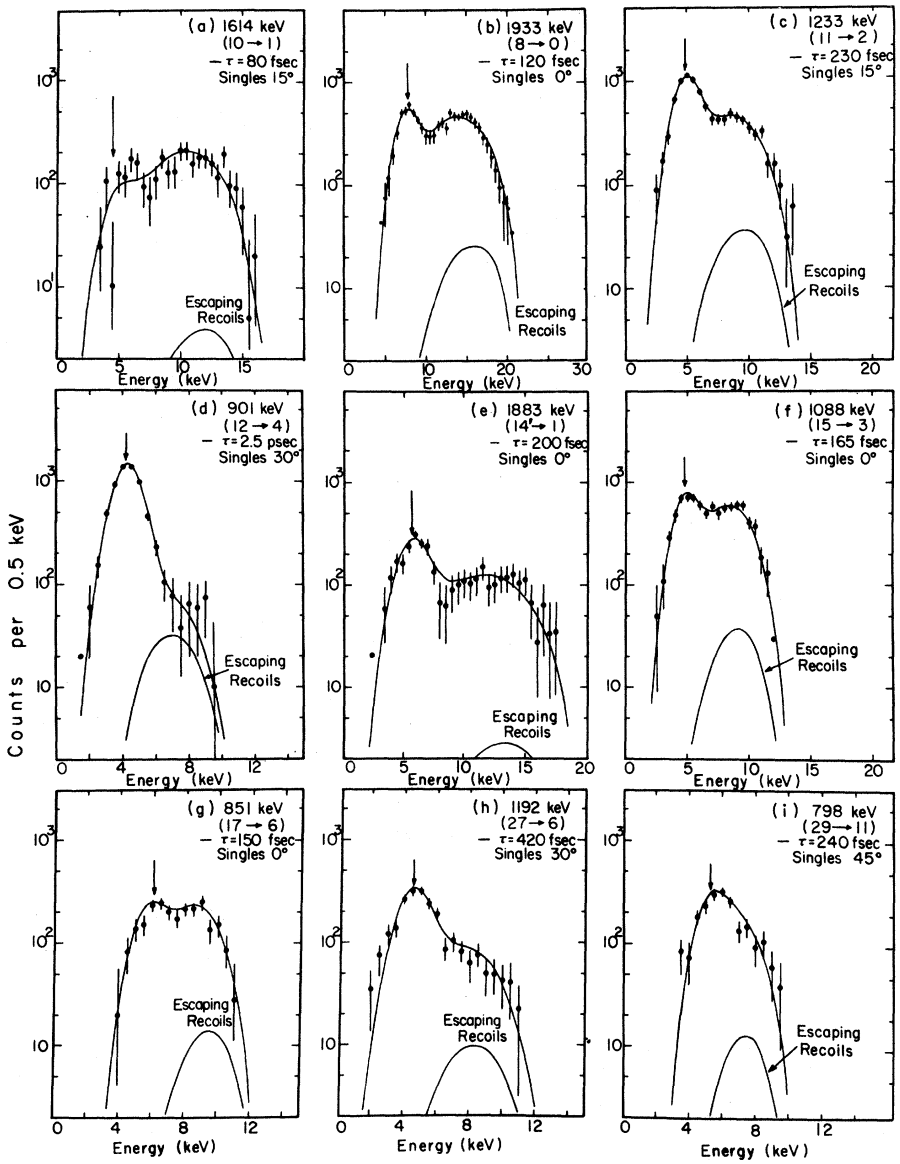

FIG. 7. Theoretical line shapes that give the minimum χ^2 values to the DSA data for nine typical transitions shown from singles measurements at 9.7 MeV. The vertical arrows point out the position of the unshifted γ ray in each case. The contribution of the escaping recoils to the Doppler shift becomes increasingly more pronounced for levels with progressively longer lifetimes.

TABLE IV. Summary of the lifetimes for levels in ^{61}Cu measured by the Doppler-shift attenuation method from singles and coincidence experiments.

Level No.	E_{level} (keV)	τ (fsec) [a] Heusch *et al.* (Ref. 12)	γ rays used in the DSA measurements in this work	τ (fsec) [a] coincidence (BRF) [c]	τ (fsec) [a] singles (BRF) [c]	τ (fsec) [a] coincidence (WU) [d]	τ (fsec) [a] singles (WU) [d]	τ (fsec) [b] adopted value
1	475.0	870^{+600}_{-300}	475.0	950^{+220}_{-170}		950 ± 100		950 ± 130
2	970.0	650^{+350}_{-190}	970.0	950^{+200}_{-180}		1040^{+250}_{-170}		990^{+185}_{-160}
3	1310.4	650^{+280}_{-170}	1310.4	760 ± 71				760 ± 104
4	1394.1	1400^{+1200}_{-500}	1394.1	1230 ± 180				1230 ± 200
5	1660.2	195 ± 30	1660.2	246 ± 18	262 ± 15 [e]		274 ± 15	263 ± 28
6	1732.5	1000^{+600}_{-300}	1732.5	≥2000				≥2000
7	1904.1	135 ± 30	1904.0, 934.1	260 ± 24	266 ± 20 [e]	242 ± 35	260 ± 10	260 ± 27
8	1932.6	67 ± 20	1932.6				126 ± 5	126 ± 14
9	1942.4	650^{+650}_{-250}	1942.4	1800^{+1600}_{-600}				1800^{+1600}_{-600}
10	2088.7	44^{+32}_{-27}	2088.9, 1613.7	56 ± 10	50 ± 3		71 ± 6	57 ± 6
11	2203.3		1233.3, 892.8			297^{+38}_{-30}	236 ± 15	250 ± 29
12	2295.0		900.8	≥2000			2600^{+800}_{-500}	2600^{+800}_{-500}
13	2336.2		1366.4, 1025.8		810 ± 174 [e]	566 ± 36	629 ± 18	621 ± 64
14	2358.1		697.6				284 ± 22	284 ± 35
15	2398.9		1429.9, 1088.4		262 ± 22 [e]		164 ± 11	174 ± 20
16	2472.3		1997.3	117 ± 23	114 ± 7		102 ± 6	108 ± 12
17	2583.6		850.9				147 ± 9	147 ± 17
18	2584.5		2584.5		142 ± 11			142 ± 18
19	2611.8		879.3, 669.3			394 ± 41	430 ± 47	411 ± 51
20	2626.8		1316.7				≥500	≥500
21	2684.0		2683.8, 2209.0		122 ± 12			122 ± 17
22	2720.2		1409.9		≥2000		≥4000	≥4000
23	2728.0		1417.8		408 ± 72		292 ± 35	329 ± 46
24	2792.5		2792.5		168 ± 24			168 ± 29
27	2923.9		1191.8			349 ± 60	402 ± 40	389 ± 51
28	2932.5		2457.6		94 ± 15			94 ± 18
29	3001.5		798.0				250^{+47}_{-80}	250^{+53}_{-84}
30	3015.6		1705.4			389 ± 40	509^{+60}_{-100}	425^{+54}_{-58}
31	3019.2		2543.9		100 ± 12			100 ± 16
32	3065.5		3065.5		57 ± 7			57 ± 9
33	3092.0		3092.0		47 ± 5			47 ± 7
35	3259.5		647.9				505^{+52}_{-45}	505^{+72}_{-68}

[a] The errors indicated are only due to statistics.

[b] Values obtained as weighted average using only statistical weights. The errors indicated include a 10% uncertainty due to the calibration of the stopping power of Ni.

[c] Experiments done by the Bartol Research Foundation group.

[d] Experiments done by the Washington University group.

[e] Values obtained by analyzing the results without decay from higher-lying states. Since some feeding was observed for these levels the values are higher than expected.

show the theoretical correlations that give the best fit for alternate spin sequences which in turn have been rejected as unlikely with high degree of confidence as discussed in Sec. IV.

D. Lifetime Measurements

Extensive measurements of the lifetimes for the ^{61}Cu levels were performed both by singles and coincidence DSA experiments. Whenever possible two γ rays deexciting a level were employed and the results were averaged. It is apparent that in general the coincidence DSA experiments are of lower statistical quality, but compared to singles data are free of uncertainties arising from possibly unknown population of the level in question through decay from higher-lying states. Although all the singles measurements were properly analyzed by accounting for observed feeding via higher-lying levels the possibility of small unobserved branches from above cannot be excluded. However, the agreement between these two types of experiments in general was found very satisfactory.

In Fig. 6 we show a comparison of the theoretical line shapes used in the extraction of lifetimes from the data for the 1366.4-, 879.3-, and 1705.4-keV γ rays from singles spectra at the indicated angles and from coincidence experiments at 0°. It is seen that the experimental line shapes are well reproduced. The singles data displayed were obtained at 10.0 MeV with a 3.8-mg/cm^2 ^{58}Ni target which gives approximately 5% recoils escaping the target. The contribution to the shift from these recoils is shown in Figs. 6(a), 6(c), and 6(e) and it has been included in the line shape that is compared with experiment. The coincidence data shown in Figs. 6(b), 6(d), and 6(f) were obtained at 12.2 MeV with a 4.0-mg/cm^2 target of ^{58}Ni on the back of which 2.0 mg/cm^2 of Au were evaporated. The lifetimes indicated in the singles shapes of Fig. 6 correspond only to the best fit for the data at the angles indicated. Peak shapes from four angles of 0, 15, 30, and 45° and centroid shifts from seven angles ranging from 0 to 110° were analyzed to provide the values reported in this work. A comparison of singles line shapes with data for peaks with lifetimes ranging from 80 fsec to 2.5 psec is shown in Fig. 7. The overall agreement of the calculated line shapes with experiment is very good.

The deduced lifetimes from the singles and the coincidence DSA experiments are summarized in Table IV. The first two columns in Table IV give the level number and level energy, while the third column gives the values of Heusch, Cujec, and Dayras[12] which are limited to the first 10 states. The fourth column gives the γ rays used in the

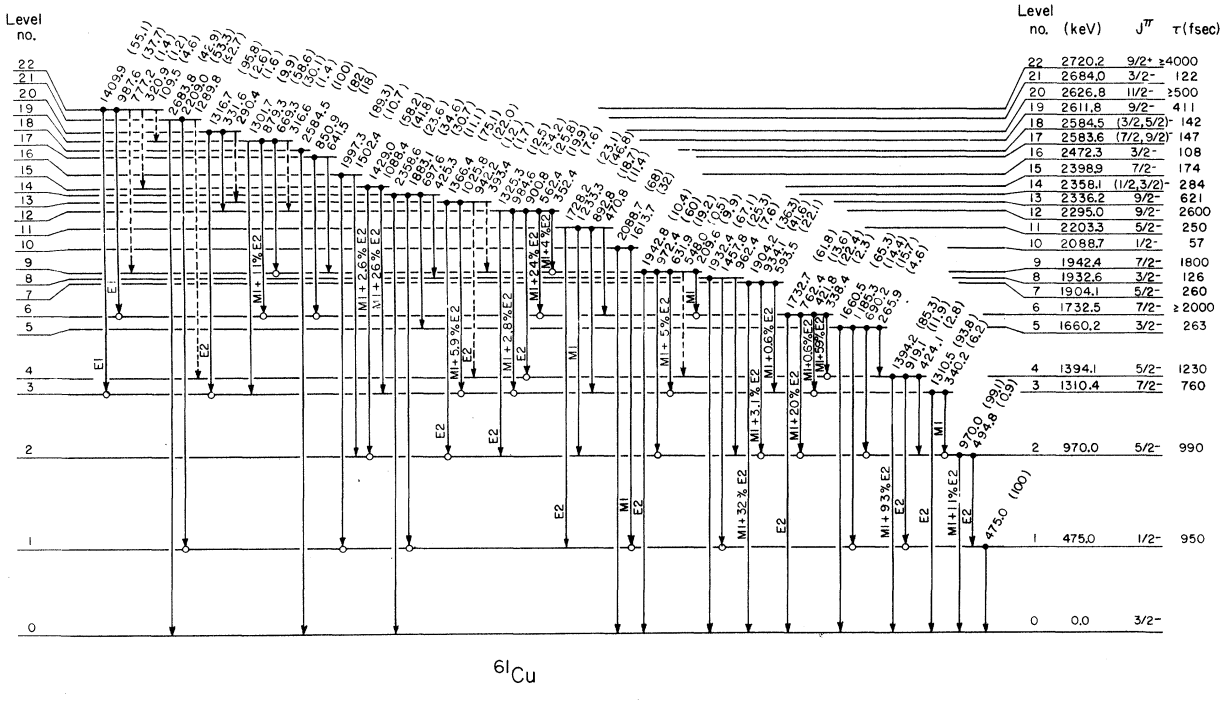

FIG. 8. Proposed scheme for the decay of levels in ^{61}Cu following excitation via the ^{58}Ni(^{4}He, $p\gamma$) reaction. Only the first 22 levels are included in this figure. The energies are in keV, the numbers in parentheses are the branching fractions for γ decay, and the level lifetimes are given in fsec (10^{-15} sec).

DSA measurements reported here, columns 5–8 give the lifetimes deduced from the coincidence and singles experiments using the tandem Van de Graaff accelerator of the University of Pennsylvania (BRF) and the cyclotron at Washington University (WU). It is clear that whenever common measurements were obtained the agreement was satisfactory. For some cases the values of column six were not corrected for feeding from above, and this resulted in longer lifetimes for the 2336.2- and 2398.9-keV levels. The last column in Table IV gives the adopted values for the mean lifetimes obtained as a weighted average from columns 5–8 using only statistical weights. An additional error of 10%, which reflects the uncertainty of the calibration[11] of the stopping power of Ni, was included in the adopted values. It is further seen that the values of Heusch, Cujec, and Dayras[12] are on the average 30% lower. Approximately $\frac{2}{3}$ of this discrepancy can be accounted for by the fact that Heusch, Cujec, and Dayras[12] employed the LSS values for the stopping power, rather than the reduced $f_n = f_e = 0.84$ values.

IV. PROPOSED DECAY SCHEME AND ASSIGNMENT OF J^π VALUES

On the basis of the evidence accumulated in this work, a detailed scheme for the decay of 44 levels in ^{61}Cu was constructed and it is shown in Figs. 8 and 9. Many of the levels in ^{61}Cu and their decay have been rather well established from Refs. 7 and 8. Here we will discuss only changes and further assignments of J^π values to levels in ^{61}Cu and of multipole mixing ratios δ for the more intense transitions in ^{61}Cu. In what follows spin sequences which are excluded without giving the confidence limit had minimum χ^2 values larger than that of a 0.1% probability for a good fit and were rejected to a better than 99.9% confidence limit. Sequences considered unlikely had lower confidence limits of rejection as indicated in each case.

The decay of the first five levels in ^{61}Cu have been well established[7,8] together with the J^π values summarized in Table I. In this work improved branching ratios were obtained while the $E2$ character of the 1310.5- and 919.2-keV transitions was confirmed. Furthermore $\delta(E2/M1)$ values obtained in this work confirm the almost pure $M1$ character of the 340.2-keV transition and the strong $E2$ admixture in the 1394.1-keV transition.[7,8]

The $\frac{7}{2}^-$ 1732.5-keV level was found to deexcite by another 338.4-keV γ ray which was observed in coincidence with the 1394.1-keV γ ray. Values for $\delta(E2/M1)$ for the transitions at 762.4, 421.8, and 338.4 keV were obtained by the ratio method, assuming[7,8] the 1732.5-keV transition to be pure $E2$

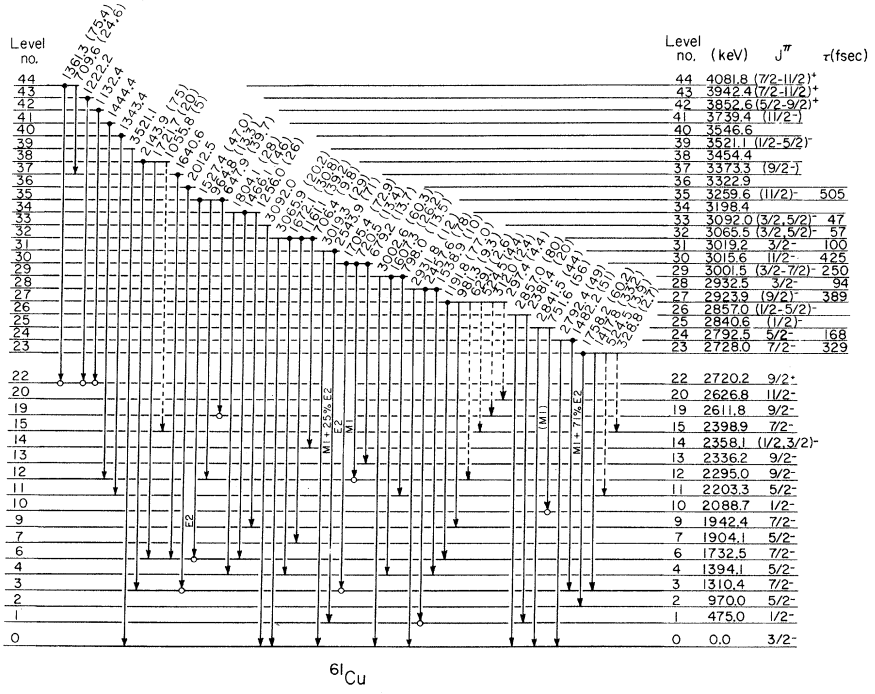

FIG. 9. Proposed scheme for the decay of levels in ^{61}Cu following excitation via the ^{58}Ni(^{4}He, $p\gamma$) reaction. Only levels Nos. 23 through 44 are shown together with those below No. 22 which are populated in their decay. The energies are in keV, the numbers in parentheses are the branching fractions for γ decay and the lifetimes are in fsec (10^{-15} sec).

in character.

The 1904.1-keV level is now definitely established as $\frac{5}{2}^-$ since the singles correlation for the ground-state transition is consistent with a $\frac{5}{2}^- \rightarrow \frac{3}{2}^-$ sequence [Fig. 3(f)], while a $\frac{3}{2}^- \rightarrow \frac{3}{2}^-$ sequence is excluded. Additional values of $\delta(E2/M1)$ for the transitions at 593.5, 934.1, and 1904.1 keV have been obtained which are in good agreement with previous measurements.[7,8]

The 1932.6-keV level is well established[7,8] as $\frac{3}{2}^-$. Here an additional weak transition at 962.4 keV from this level is proposed on grounds of good energy agreement. More accurate values for $\delta(E2/M1)$ for the 1932.6-keV transition have been obtained (see Table III) and these are in good agreement with the limits placed by Heusch *et al.*[7]

The 1942.35-keV level was assigned[8] as $\frac{7}{2}^-$ and this is further supported by the present work by the small $\delta(M3/E2)$ value of $-(0.08^{+0.15}_{-0.12})$ obtained from the 1942.35-keV correlation. The large uncertainties on this value are due to difficulties in resolving this γ ray from the highly Doppler-shifting and interfering 1932.6-keV peak. The present $\delta(E2/M1)$ values for the 209.6- and 631.9-keV transitions (Table III) are somewhat different than previous results from Refs. 7 and 8. A weak branch at 548.0 keV was tentatively assigned to deexcite this level on energy grounds, while a better branching ratio[7,8] for the 972.4-keV γ ray was obtained by actually resolving the (970.0, 972.4)-keV doublet. The 2088.7-keV level was established[8] as $\frac{1}{2}^-$.

For the level at 2203.25 keV, we can limit its J^π value to $\frac{5}{2}^-$. The singles correlation for the 1233.3-keV γ ray [Fig. 3(l)] excludes a $\frac{9}{2}^- \rightarrow \frac{5}{2}^-$ or a $\frac{3}{2}^- \rightarrow \frac{5}{2}^-$ sequence, while the correlation for the 892.8-keV γ ray [Fig. 3(j)] makes the $\frac{7}{2}^- \rightarrow \frac{7}{2}^-$ sequence unlikely (rejected at a 90% confidence level). Two additional γ rays at 470.8 and 1728.2 keV have been assigned on grounds of good energy agreement to deexcite this level.

For the 2295.0-keV level considerably improved[7,8] branching ratios were obtained by resolving a (984.6, 987.6)-keV doublet (Fig. 2). The 984.6-keV γ ray was further observed in coincidence with the 1310.4-keV γ ray, which places it to deexcite this level. Another weaker branch at 1325.3 keV was assigned here on energy grounds. The $\frac{9}{2}^-$ assignment[8] for the 2295.0-keV level is confirmed in this work from the correlations for the 562.4-, 900.8-, and 984.6-keV γ rays [Figs. 4(d), 4(b), and 4(a)] which are consistent only with a $\frac{9}{2}^-$ assignment for this level. The δ values obtained for the γ rays at 352.4, 562.4, and 984.6 keV are in good agreement with earlier results.[8] The 900.8-keV γ ray was further found to be consistent with a pure $E2$ transition as evinced by the small (0.026 ± 0.062) value for $\delta(M3/E2)$ for this transition.

The level at 2336.2 keV is now definitely assigned as $\frac{9}{2}^-$ on the basis of the singles correlations for the 1366.4- and 1025.8-keV transitions [Figs. 4(e) and 4(f)]. These γ rays have been established to deexcite this level, since they were observed in coincidence with the 970.0- and 1310.4-keV γ rays, respectively (Table II). The 1366.4-keV transition is found to be pure $E2$ in character, since $\delta(M3/E2) = 0.022 \pm 0.024$. Two additional weak branches are tentatively proposed to deexcite this level at 393.4 and 942.2 keV on grounds of good energy agreement.

The population of a level at 2358.1 keV in the decay of ^{61}Zn has been independently verified in Refs. 5 and 6 with consistent branching ratios as shown in Table I. However, in the present studies four γ rays at the same energies[5,6] of 425.3, 697.6, 1883.1, and 2358.6 keV have been consistently found in the 10.0-MeV (^{4}He, $p\gamma$) experiments to have the following different branching ratios of (7.6 ± 0.9), (9.9 ± 0.9), (59.6 ± 2.2), and (17.8 ± 0.9)%, respectively. This indicates either the fortuitous existence of at least three of these γ rays at 425.3, 1883.1, and 2358.6 keV from other unidentified levels, or the presence of two close levels at 2358.1 keV. Furthermore, the lifetimes of the 697.6- and 1883.1-keV γ rays were found to be 284 ± 22 and 186 ± 8 fsec, respectively. This result in conjunction with the branching ratios given above make it likely that the 697.6-keV γ ray is primarily associated with the level formed in the ^{61}Zn decay, while the 1883.1-keV γ ray originates primarily from a different level. This tentative level has not been incorporated in the scheme of Fig. 8. In view of the possibility of two close levels at this energy, the J^π assignment for the level from radioactivity can be limited only to $(\frac{1}{2}-\frac{5}{2})^-$. The 1883.1-keV γ ray has a singles correlation with a large negative A_2 term and if it is assumed to decay to the $\frac{1}{2}^-$ level at 475.0 keV then it must come from a $\frac{3}{2}^-$ level.

For the level at 2398.9 keV a $\frac{7}{2}^-$ assignment was proposed.[8] This is confirmed in the present work on the basis of the correlations for the 1088.4- and 1429.0-keV transitions [Figs. 4(g) and 4(h)] which show that all possibilities other than $\frac{7}{2}^-$ for this level can be excluded. The δ value of 0.164 ± 0.024 for the 1429.0-keV transition obtained in this work is in disagreement with the earlier result[8] of $0.82 \leq \delta \leq 1.7$.

The levels at 2472.3, 2684.0, and 2932.5 keV have been previously[8] assigned as $\frac{3}{2}^-$ and this is confirmed in the present work.

In Ref. 8 a level at 2583.7 keV was assigned to deexcite via two γ rays at 850.9 and 2584.5 keV. In this work we find that the relative cross section for these two γ rays varies with bombard-

ment energy and this suggests that these γ rays originate from different levels in ^{61}Cu. A level at 2583.6 keV was assigned to deexcite via the 850.9-keV γ ray which was seen in coincidence with the 421.9- and 1732.5-keV γ rays, and via the 641.5-keV γ ray on good energy agreement. The singles correlation for the 850.9-keV γ ray has a definite maximum at 90° and this eliminates a $\frac{1}{2}^-$ or $\frac{3}{2}^-$ assignment for the 2583.6-keV level. Arguments in favor of a $\frac{7}{2}^-$ or $\frac{9}{2}^-$ assignment for this level can be given from the energy dependence of the yield[9,10] for the 850.9-keV γ ray. The 2584.5-keV singles correlation has a definite maximum at 90° and this excludes a $\frac{1}{2}^-$ or $\frac{7}{2}^-$ assignment for the 2584.5-keV level leaving a $\frac{3}{2}^-$ or $\frac{5}{2}^-$ as possibilities.

The level at 2611.8 keV was assigned as $\frac{9}{2}^-$ in Ref. 8 and this is consistent with the present results. The two γ rays at 669.3 and 879.3 keV were established to deexcite this level, since they were observed in coincidence with the 631.9- and 421.8-keV γ rays, respectively (Table II). The correlations for the 669.3- and 879.3-keV γ rays were found consistent only with $\frac{9}{2}^- \rightarrow \frac{7}{2}^-$ or $\frac{5}{2}^- \rightarrow \frac{7}{2}^-$ sequences [Figs. 4(j) and 4(l)]. However, the fact that (i) this level is not populated in the ^{61}Zn decay and (ii) that it has a high yield of population[10] at high bombardment energy (20 MeV) help eliminate the $\frac{5}{2}^-$ value as a possibility. Two additional weak branches at 316.6 and 1301.7 keV are also proposed from this level.

A level at 2626.8 keV reported[8] earlier was confirmed in this work by the observed coincidence of the 1316.7-keV γ ray with the γ rays at 340.2 and 1310.4 keV. Two additional γ rays at 331.6 and 290.4 keV were assigned on energy grounds to deexcite this level, but a γ ray at 229.6 keV reported[8] earlier was not observed in this work. The singles correlation for the 1316.7-keV γ ray [Fig. 4(k)] is only consistent with an $\frac{11}{2}^- \rightarrow \frac{7}{2}^-$ or $\frac{7}{2}^- \rightarrow \frac{7}{2}^-$ sequence for this transition. A study of the relative yields of the levels in ^{61}Cu as a function of bombardment energy[10] indicates that a $\frac{7}{2}^-$ assignment for this level is very unlikely. We limit, therefore, the J^π value for this level to $\frac{11}{2}^-$.

A level at 2720.2 keV was assigned as $\frac{9}{2}^+$ in Ref. 8, and it was identified with the level at 2711 keV observed[28] in the (^{3}He, d) reaction with an $l_p = 4$ transfer. This assignment is firmly established from the present results. The $l_p = 4$ transfer limits J^π to $\frac{7}{2}^+$ or $\frac{9}{2}^+$ for a level that could be identified with the 2720.6- or the 2728.0-keV level. The latter possibility is excluded because it would require a $\frac{9}{2}^+ \rightarrow \frac{5}{2}^-$ sequence for the 1758.2-keV transition ($M2$ in character) or a $\frac{7}{2}^+ \rightarrow \frac{5}{2}^-$ sequence for which a value of $\delta(M2/E1) = 1.55^{+0.34}_{-0.30}$ would be required from the correlation [Fig. 5(d)] for the 1758.2-keV γ ray, and both of these are extremely unlikely. This identifies the $\frac{7}{2}^+$ or $\frac{9}{2}^+$ level from the (^{3}He, d) reaction with the 2720.2-keV level. The 987.6- and 1409.9-keV γ rays were observed in coincidence with the 1310.4- and 1732.5-keV γ rays, respectively (Table II), thus establishing them to deexcite the 2720.6-keV level. Now a $\frac{7}{2}^+ \rightarrow \frac{7}{2}^-$ sequence for the 1409.9-keV transition is excluded on the basis of the correlation for this transition [Fig. 5(a)]. This establishes both the 1409.9- and 987.6-keV transitions as $E1$ in character with a sequence of $\frac{9}{2}^+ \rightarrow \frac{7}{2}^-$, for which $\delta(M2/E1)$ ratios of 0.035 ± 0.030 and 0.00 ± 0.03, respectively, were obtained. Additional weak branches at 109.5, 320.9, and 777.2 keV are tentatively proposed for this level on grounds of good energy agreement.

The level at 2728.0 keV proposed in Ref. 8 is confirmed here and it is definitely assigned as $\frac{7}{2}^-$. From the correlation of the 1758.2-keV γ ray [Fig. 5(d)] all sequences except the $\frac{7}{2}^- \rightarrow \frac{5}{2}^-$ can be excluded for this transition. Two weak γ rays at 382.8 and 524.5 keV are tentatively proposed on energy grounds to deexcite this level.

The 2792.5-, 2840.6-, 2857.0-, 3001.5-, 3322.9-, 3521.1-, and 3546.6-keV levels have been well characterized previously[8] and for these only improved branching ratios are reported here (Table I).

A level at 2923.9 keV proposed[8] to deexcite by a 1191.8-keV γ ray is confirmed here and five additional γ rays are tentatively proposed to depopulate this level on grounds of good energy agreement. The singles correlation for the 1191.8-keV γ ray [Fig. 5(e)] excludes a $\frac{3}{2}^-$ or $\frac{11}{2}^-$ assignment and permits one to reject the $\frac{7}{2}^-$ possibility at the 90% confidence level. Of the two remaining possibilities $\frac{5}{2}^-$ and $\frac{9}{2}^-$ we suggest the $\frac{9}{2}^-$ as the most likely since this level does not decay to levels with $J \leq \frac{5}{2}^-$ and has a high yield of population[10] at 20 MeV.

The level at 3015.6 keV was firmly established in this work by observing the 1705.4- and 720.5-keV γ rays in coincidence with the 1310.4- and the 562.4-keV γ rays, respectively. The 679.2-keV γ ray was also assigned[8] on energy grounds to deexcite this level. The singles correlations for the 1705.4- and 720.5-keV γ rays exclude a $\frac{3}{2}^-$, $\frac{5}{2}^-$, or $\frac{9}{2}^-$ assignment for this level but they are both consistent with an $\frac{11}{2}^-$ or $\frac{7}{2}^-$ assignment. The unusually high yield of population of this level at higher bombarding energies[10] makes a $\frac{7}{2}^-$ assignment unlikely leaving the $\frac{11}{2}^-$ assignment as the most likely one.

The level at 3019.2 keV is established as $\frac{3}{2}^-$ in this work on the basis of the correlation for the 2543.9-keV γ ray [Fig. 5(g)] which populates the $\frac{1}{2}^-$ at 475.0 keV and shows a definite maximum

at 90°.

The level at 3065.5 keV was assigned to deexcite by two additional γ rays at 706.4 and 1161.1 keV to levels J^π of $\frac{5}{2}^-$ and $(\frac{1}{2}, \frac{3}{2})^-$, respectively, on energy grounds. Both the 706.4- and 1672.1-keV correlations peak at 90° and this limits the J^π value for this level to $\frac{3}{2}^-$ or $\frac{5}{2}^-$.

The 3092.0-keV level deexcites only to the ground state and its correlation peaks at 90° which limits J^π for this level to $(\frac{3}{2}, \frac{5}{2})^-$.

The levels at 3198.4 and 3454.4 keV have been established[8] from $p\gamma$-coincidence information. The proposed decay mode for these levels is shown in Table I, but the J^π values for these levels cannot be determined from the present limited information.

A level at 3259.6 keV was reported[8] to deexcite via transitions at 1527.0 and 1599 keV. In this work a 1599-keV γ ray was not observed. Two γ rays at 647.9 and 1527.4 keV were observed in coincidence with the 879.3- and 1732.5-keV γ rays, respectively. This establishes the decay of this 3259.6-keV level via the 647.9- and 1527.4-keV transitions. An additional tentative γ ray at 964.8 keV has been assigned on energy grounds. This level was observed to decay only to $\frac{7}{2}^-$ and $\frac{9}{2}^-$ levels below thus suggesting a high J^π value for this level. Again the high yield[10] of population of this level at 20 MeV supports an $\frac{11}{2}^-$ assignment.

A level at 3373.3 keV is confirmed[8] to decay only via the 1640.6-keV transition to the $\frac{7}{2}^-$ 1732.5-keV level. The high yield for the level[10] at 20-MeV bombardment energy favors a $\frac{9}{2}^-$ assignment.

A level at 3739.4 keV deexciting by the 1444.4-keV γ ray is proposed here on the basis of (i) a level at 3748 ± 7 keV observed in the proton spectra,[8] (ii) an observed coincidence of the 1444.4-keV γ ray with protons[8] corresponding to 3500–3750 keV of excitation in ^{61}Cu, and (iii) yield information[10] strongly supporting an $\frac{11}{2}^-$ assignment for a level at such an excitation. Decay to other states with $J \geq \frac{7}{2}$ in the range 2100–2260 keV is not possible since only the sum 2295.0 + 1444.4 leads to an observed level.[8]

A level at 3852.4 keV is confirmed[8] and two new levels at 3942.4 and 4081.8 keV are established in this work on the basis of observed coincidences of the 1132.4-, 1222.2-, and 1361.3-keV γ rays with the 1409.9-keV γ ray. Since these three levels decay to the $\frac{9}{2}^+$ level their J^π values are likely to be $\frac{7}{2}^+$, $\frac{9}{2}^+$, or $\frac{11}{2}^+$, although $\frac{5}{2}^+$ or $\frac{13}{2}^+$ cannot be excluded. The yield information[10] for these levels at 20 MeV favors a $(\frac{9}{2}, \frac{7}{2}, \frac{5}{2})^+$ assignment for the 3852.6-keV level, $(\frac{11}{2}, \frac{9}{2}, \frac{7}{2})^+$ for the 3942.4-keV level, and $(\frac{11}{2}, \frac{9}{2})^+$ for the 4081.8-keV level.

Levels at 3276, 3578, 3597, 3618, 3646, 3686, 3748, 3802, 3943, and 3978 keV were observed[8] in the high-resolution proton spectra and were assigned[8] to decay by the γ rays summarized in Table 3 of Ref. 8. Of these, the γ rays at 648.8, 709.6, and 1222.2 keV were assigned from coincidence information and better energy agreement to deexcite levels at 3259.6, 4081.8, and 3942.4 keV rather than 3277, 3802, and 3950 keV reported in Ref. 8. Of the remaining γ rays assigned in Ref. 8 to deexcite the above levels we did not observe γ rays at 1074, 956, 2273, 3116, 2302, 1492, and 2406 keV to be associated with the ^{58}Ni(^{4}He, $p\gamma$) reaction. The remaining weak γ rays at 2611, 832, and 790 keV were observed but no evidence for definite assignment of these γ rays to deexcite the above levels could be found in this work. Furthermore, we should mention that the γ-ray spectra obtained at the 12.2-MeV experiments exhibited a considerable number of additional unidentified γ rays with energies as high as 4800 keV. We made no effort to assign these to new levels, and found no place for them between levels already established in this work via $p\gamma$- and $\gamma\gamma$-coincidence experiments.

V. DISCUSSION

A. Reduced Transition Probabilities

From the measured branching ratios, multipole mixing ratios, and the level lifetimes presented in Tables I, III, and IV we can deduce the reduced transition probabilities $B(E2)$ and $B(M1)$ for the electric quadrupole and magnetic dipole components of 46 transitions from 21 levels in ^{61}Cu with well-established J^π values. These results are summarized in Table V where the first column gives the transition between levels as numbered in Table I, the second column gives the transition energy in keV, the third column gives the established $J^\pi_i \to J^\pi_f$ sequence with subscripts indicating the order of appearance of each J^π value, the fourth and sixth columns give the $B(E2)$ and $B(M1)$ values in units of $e^2\,\mathrm{fm}^4$ and $e^2\,\mathrm{fm}^2$, respectively, and the fifth and seventh columns give the $B(E2)$ and $B(M1)$ values in Weisskopf units (W.u.) obtained via the expressions given in the Appendix.

First, we point out that the more accurate $B(E2)$ values were obtained for those transitions that are pure $E2$ in character. For many of the other $B(E2)$ entries in Table V the major contribution to the uncertainties originates from the multipole mixing ratios. On the other hand, more accurate values for the $B(M1)$ values are normally obtained with few exceptions for transitions with large $E2$ admixtures.

Before comparing the present results with theory it is instructive to attempt to classify and corre-

TABLE V. Electromagnetic transition rates in ^{61}Cu.

Transition	E_γ (keV)	$J^\pi_i \to J^\pi_f$	$B(E2)$ values (e^2 fm^4)	$B(E2)$ values (W.u.)	$B(M1)$ values (e^2 fm^2)	$B(M1)$ values (W.u.)
1→0	475.0	$\frac{1}{2_1}^- \to \frac{3}{2_1}^-$	57 ± 8	4.0 ± 0.5	$(6.2 \pm 0.8) \times 10^{-3}$	0.32 ± 0.04
2→0	970.0	$\frac{5}{2_1}^- \to \frac{3}{2_1}^-$	104 ± 23	7.3 ± 1.6	$(6.2 \pm 1.0) \times 10^{-4}$	0.031 ± 0.005
2→1	494.8	$\frac{5}{2_1}^- \to \frac{1}{2_1}^-$	251 ± 50	18 ± 3		
3→0	1310.5	$\frac{7}{2_1}^- \to \frac{3}{2_1}^-$	261 ± 36	18 ± 2		
3→2	340.2	$\frac{7}{2_1}^- \to \frac{5}{2_1}^-$	$3.7^{+6.1}_{-3.7}$	$0.26^{+0.42}_{-0.26}$	$(1.3 \pm 0.2) \times 10^{-3}$	0.066 ± 0.009
4→0	1394.1	$\frac{5}{2_2}^- \to \frac{3}{2_1}^-$	100 ± 17	7.0 ± 1.1	$(1.2 \pm 0.2) \times 10^{-5}$	$(6.0 \pm 1.1) \times 10^{-4}$
4→1	919.1	$\frac{5}{2_2}^- \to \frac{1}{2_1}^-$	121 ± 21	8.5 ± 1.5		
5→0	1660.2	$\frac{3}{2_2}^- \to \frac{3}{2_1}^-$	105^{+17}_{-22} or 21^{+17}_{-10}	$7.4^{+1.2}_{-1.5}$ or $1.5^{+1.2}_{-0.7}$	$(1.2^{+0.4}_{-0.3}) \times 10^{-4}$ or $(3.0^{+0.4}_{-0.5}) \times 10^{-4}$	$(6.0^{+2.2}_{-1.5}) \times 10^{-3}$ or $0.015^{+0.002}_{-0.003}$
5→1	1185.3	$\frac{3}{2_2}^- \to \frac{1}{2_1}^-$	8–85	0.6–5.9	$(0.7–1.7) \times 10^{-4}$	$(3.5–8.6) \times 10^{-3}$
5→2	690.3	$\frac{3}{2_2}^- \to \frac{5}{2_1}^-$	≤89 or 2820 ± 370	≤6.5 or 198 ± 26	$(1.14 \pm 0.15) \times 10^{-3}$ or $(1.08^{+0.15}_{-0.17}) \times 10^{-4}$	0.058 ± 0.008 or $(5.5^{+0.8}_{-0.9}) \times 10^{-3}$
6→0	1732.5	$\frac{7}{2_2}^- \to \frac{3}{2_1}^-$	≤17	≤1.6		
6→2	762.5	$\frac{7}{2_2}^- \to \frac{5}{2_1}^-$	≤48	≤3.4	$\leq 8.4 \times 10^{-5}$	$\leq 4.2 \times 10^{-3}$
6→3	421.8	$\frac{7}{2_2}^- \to \frac{7}{2_1}^-$	≤74	≤5.1	$\leq 1.1 \times 10^{-3}$	≤0.054
6→4	338.4	$\frac{7}{2_2}^- \to \frac{5}{2_2}^-$	≤1720	≤120	$\leq 1.5 \times 10^{-4}$	$\leq 7.5 \times 10^{-3}$
7→0	1904.2	$\frac{5}{2_3}^- \to \frac{3}{2_1}^-$	15^{+3}_{-2}	1.0 ± 0.2	$(8.7^{+1.1}_{-1.2}) \times 10^{-5}$	$(4.6^{+0.6}_{-0.7}) \times 10^{-3}$
7→2	934.1	$\frac{5}{2_3}^- \to \frac{5}{2_1}^-$	58 ± 17	4.0 ± 1.2	$(1.20 \pm 0.13) \times 10^{-3}$	0.061 ± 0.007
7→3	593.5	$\frac{5}{2_3}^- \to \frac{7}{2_1}^-$	54^{+29}_{-32}	$3.8^{+2.0}_{-2.2}$	$(2.6 \pm 0.3) \times 10^{-3}$	0.13 ± 0.02
8→0	1932.6	$\frac{3}{2_3}^- \to \frac{3}{2_1}^-$	10^{+9}_{-5} or 124^{+24}_{-18}	$0.72^{+0.63}_{-0.35}$ or $8.7^{+1.6}_{-1.3}$	$(4.4 \pm 0.6) \times 10^{-4}$ or $(1.1^{+0.3}_{-0.5}) \times 10^{-4}$	0.022 ± 0.003 or $(5.9^{+1.7}_{-3.0}) \times 10^{-3}$
8→1	1475.8	$\frac{3}{2_3}^- \to \frac{1}{2_1}^-$	224 ± 31 or $9.5^{+6.7}_{-7.5}$	16 ± 2 or $0.67^{+0.46}_{-0.51}$	$(4.1 \pm 1.6) \times 10^{-5}$ or $(3.9 \pm 0.5) \times 10^{-4}$	$(2.1 \pm 0.8) \times 10^{-3}$ or 0.020 ± 0.003
9→0	1942.4	$\frac{7}{2_3}^- \to \frac{3}{2_1}^-$	$1.7^{+0.9}_{-0.8}$	$0.12^{+0.06}_{-0.05}$		
9→3	631.9	$\frac{7}{2_3}^- \to \frac{7}{2_1}^-$	43^{+47}_{-38}	$3.0^{+3.3}_{-2.6}$	$(2.5^{+1.3}_{-1.2}) \times 10^{-4}$	0.013 ± 0.007
9→6	209.6	$\frac{7}{2_3}^- \to \frac{7}{2_2}^-$	≤730	≤51	$(3.7^{+1.9}_{-1.8}) \times 10^{-3}$	$0.19^{+0.10}_{-0.09}$
10→1	1613.7	$\frac{1}{2_2}^- \to \frac{1}{2_1}^-$			$(8.4 \pm 1.2) \times 10^{-4}$	0.043 ± 0.006
11→1	1728.2	$\frac{5}{2_4}^- \to \frac{1}{2_1}^-$	48.9 ± 6.4	3.4 ± 0.4		
11→2	1233.3	$\frac{5}{2_4}^- \to \frac{5}{2_1}^-$	$0.5^{+0.8}_{-0.5}$	$0.03^{+0.05}_{-0.03}$	$(6.3 \pm 1.1) \times 10^{-4}$	0.032 ± 0.006

TABLE V *(Continued)*

Transition	E_γ (keV)	$J^\pi_i \to J^\pi_f$	$B(E2)$ values (e^2 fm^4)	$B(E2)$ values (W.u.)	$B(M1)$ values (e^2 fm^2)	$B(M1)$ values (W.u.)
11→3	892.8	$\frac{5}{2_4}^- \to \frac{7}{2_1}^-$	≤1.7 or 1065 ± 130	≤0.088 or 75 ± 9	$(6.6 \pm 0.8)\times10^{-4}$ or $(7.8^{+6.7}_{-4.5})\times10^{-6}$	0.034 ± 0.004 or $(3.9 \pm 3.4)\times10^{-4}$
12→2	1325.3	$\frac{9}{2_1}^- \to \frac{5}{2_1}^-$	9.6 ± 2.3	0.67 ± 0.16		
12→3	987.6	$\frac{9}{2_1}^- \to \frac{7}{2_1}^-$	$3.3^{+1.3}_{-1.4}$	$0.23^{+0.09}_{-0.10}$	$(8.5 \pm 2.0)\times10^{-5}$	$(4.3^{+0.9}_{-1.1})\times10^{-3}$
12→4	900.8	$\frac{9}{2_1}^- \to \frac{5}{2_2}^-$	137 ± 32	9.6 ± 2.2		
12→6	562.4	$\frac{9}{2_1}^- \to \frac{7}{2_2}^-$	265 ± 64	19 ± 4	$(2.1 \pm 0.5)\times10^{-4}$	0.010 ± 0.002
12→9	352.4	$\frac{9}{2_1}^- \to \frac{7}{2_3}^-$	169^{+150}_{-107}	12^{+11}_{-8}	$(4.1 \pm 1.0)\times10^{-4}$	0.020 ± 0.005
13→2	1366.4	$\frac{9}{2_2}^- \to \frac{5}{2_1}^-$	207 ± 22	14.5 ± 1.5		
13→3	1025.8	$\frac{9}{2_2}^- \to \frac{7}{2_1}^-$	$15.0^{+10.0}_{-7.8}$	$1.05^{+0.71}_{-0.56}$	$(1.95 \pm 0.23)\times10^{-4}$	$(9.9 \pm 1.2)\times10^{-3}$
13→4	942.2	$\frac{9}{2_2}^- \to \frac{5}{2_2}^-$	21 ± 4	1.49 ± 0.29		
15→2	1429.0	$\frac{7}{2_4}^- \to \frac{5}{2_1}^-$	12.0 ± 3.8	0.84 ± 0.26	$(7.1 \pm 0.9)\times10^{-4}$	0.036 ± 0.004
15→3	1088.4	$\frac{7}{2_4}^- \to \frac{7}{2_1}^-$	340^{+190}_{-302}	24^{+13}_{-21}	$(8.7^{+2.0}_{-2.8})\times10^{-4}$	$0.044^{+0.010}_{-0.014}$
16→1	1997.3	$\frac{3}{2_4}^- \to \frac{1}{2_1}^-$	≤0.6 or 92 ± 14	≤0.04 or 6.4 ± 1.0	$(6.6 \pm 0.7)\times10^{-4}$ or $(3.7 \pm 0.5)\times10^{-4}$	0.033 ± 0.004 or 0.019 ± 0.003
19→6	879.3	$\frac{9}{2_3}^- \to \frac{7}{2_2}^-$	254^{+133}_{-144}	$17.8^{+9.3}_{-8.0}$	$(1.17 \pm 0.15)\times10^{-3}$	0.059 ± 0.008
19→9	669.3	$\frac{9}{2_3}^- \to \frac{7}{2_3}^-$	262^{+85}_{-68}	18^{+6}_{-5}	$(1.45 \pm 0.18)\times10^{-3}$	0.073 ± 0.009
20→3	1316.7	$\frac{11}{2_1}^- \to \frac{7}{2_1}^-$	≤400	≤27		
23→2	1758.2	$\frac{7}{2_5}^- \to \frac{5}{2_1}^-$	63 ± 14	4.4 ± 1.0	$(6.3^{+2.1}_{-2.3})\times10^{-5}$	$(3.2^{+1.1}_{-1.2})\times10^{-3}$
23→3	1417.8	$\frac{7}{2_5}^- \to \frac{7}{2_1}^-$	≤77	≤5.3	$(2.0^{+0.6}_{-1.0})\times10^{-4}$	$0.010^{+0.003}_{-0.005}$
27→6	1191.8	$\frac{9}{2_4}^- \to \frac{7}{2_2}^-$	≤1.7	≤0.12	$(7.4 \pm 1.1)\times10^{-4}$	0.037 ± 0.005
30→3	1705.4	$\frac{11}{2_2}^- \to \frac{7}{2_1}^-$	97 ± 14	6.8 ± 1.0		
30→12	720.5	$\frac{11}{2_2}^- \to \frac{9}{2_1}^-$	≤0.7	≤0.05	$(5.3 \pm 0.0)\times10^{-4}$	0.027 ± 0.004
31→1	2543.9	$\frac{3}{2}^- \to \frac{1}{2_1}^-$	≤27	≤1.8	$(2.0^{+0.7}_{-0.8})\times10^{-4}$	0.010 ± 0.004

late the $B(E2)$ and $B(M1)$ values according to transition strength. For this purpose in Fig. 10 we summarize the results of Table V in a histogram form with the numbers indicating the spin sequences shown (e.g. $5_2 \to 3_1$ abbreviating $\frac{5}{2_2}^- \to \frac{3}{2_1}^-$). From Fig. 10 one notices that the $B(E2)$ values cluster between 2 and 20 W.u., while the $B(M1)$ values cluster between 0.01 and 0.1 W.u. Further, we observe from Fig. 10(a) that for the transitions leading to the ground state with sequences $(J_k \to \frac{3}{2_1})$ for transitions of given J, the $B(E2)$ values are highest for $k=1$ and then decrease considerably with increasing k. For transitions leading to excited states, however, no such definite correla-

TABLE VI. Comparison of experimental and theoretical $B(E2)$ and $B(M1)$ values, multipole mixing ratios $\delta(E2/M1)$, and branching ratios for the first 10 levels in ^{61}Cu.

Transition	E_γ [a] (keV)	$J^\pi_i \to J^\pi_f$	$B(E2)$ (W.u.) Theory [b]	$B(E2)$ (W.u.) Experiment [c]	$B(M1)$ (W.u.) Theory [b]	$B(M1)$ (W.u.) Experiment [c]	$\delta(E2/M1)$ Theory [b]	$\delta(E2/M1)$ Experiment [c]	Branching ratios (%) Theory [d]	Branching ratios (%) Experiment [e]
1→0	475.0	$\frac{1}{2_1}^- \to \frac{3}{2_1}^-$	11.0	4.0 ± 0.5	0.76	0.32 ± 0.04	0.04		100	100
2→0	970.0	$\frac{5}{2_1}^- \to \frac{3}{2_1}^-$	5.4	7.3 ± 1.6	4×10^{-4}	0.031 ± 0.005	2.7	0.35 ± 0.03	96	99.1 ± 0.6
2→1	494.8	$\frac{5}{2_1}^- \to \frac{1}{2_1}^-$	7.8	18 ± 3					4	0.9 ± 0.1
3→0	1310.5	$\frac{7}{2_1}^- \to \frac{3}{2_1}^-$	15.5	18 ± 2					79	93.8 ± 0.2
3→2	340.2	$\frac{7}{2_1}^- \to \frac{5}{2_1}^-$	0.01	$0.26^{+0.42}_{-0.26}$	0.22	0.066 ± 0.009	~0	$0.00^{+0.09}_{-0.07}$	21	6.2 ± 0.2
4→0	1394.1	$\frac{5}{2_2}^- \to \frac{3}{2_1}^-$	8.8	7.9 ± 1.1	0.0066	$(6.0 \pm 1.1) \times 10^{-4}$	1.2	3.54 ± 0.13	96.4	85.3 ± 2.5
4→1	919.1	$\frac{5}{2_2}^- \to \frac{1}{2_1}^-$	1.9	8.5 ± 1.5					1.5	11.9 ± 0.6
4→2	424.1	$\frac{5}{2_2}^- \to \frac{5}{2_1}^-$	1.2		0.012		0.10		2.1	2.8 ± 0.3
5→0	1660.2	$\frac{3}{2_2}^- \to \frac{3}{2_1}^-$	10.4	$7.2^{+1.2}_{-1.5}$ or $1.5^{+1.2}_{-0.7}$	0.01	$(6.0^{+2.2}_{-1.5}) \times 10^{-3}$ or $0.015^{+0.002}_{-0.003}$	1.1	$-(1.37^{+0.23}_{-0.35})$ or $-(0.39^{+0.18}_{-0.10})$	55.3	65.3 ± 1.5
5→1	1185.3	$\frac{3}{2_2}^- \to \frac{1}{2_1}^-$	0.020	0.6–5.9	0.035	$(3.5\text{–}9.5) \times 10^{-3}$	~0	$0.26 \leq \delta \leq 1.0$	28.0	14.4 ± 0.9
5→2	690.3	$\frac{3}{2_2}^- \to \frac{5}{2_1}^-$	0.61	≤6.5 or 198 ± 26	0.077	0.058 ± 0.008 or $(5.5^{+0.8}_{-0.9}) \times 10^{-3}$	0.045	$-(0.04 \pm 0.16)$ or $3.1^{+1.4}_{-0.9}$	12.1	15.7 ± 1.2
5→4	265.9	$\frac{3}{2_2}^- \to \frac{5}{2_2}^-$								4.6 ± 0.3
6→0	1732.5	$\frac{7}{2_2}^- \to \frac{3}{2_1}^-$	0.04	≤1.6					1.9	61.8 ± 3.0
6→2	762.5	$\frac{7}{2_2}^- \to \frac{5}{2_1}^-$	0.16	≤3.4	0.038	$\leq 4.2 \times 10^{-3}$	0.04	$-(0.50 \pm 0.03)$	96.4	13.6 ± 1.0
6→3	421.8	$\frac{7}{2_2}^- \to \frac{7}{2_1}^-$	0.24	≤6.7	0.003	≤0.054	0.09	$-(0.080 \pm 0.043)$	1.3	22.4 ± 3.4
6→4	338.4	$\frac{7}{2_2}^- \to \frac{5}{2_2}^-$	0.02	≤120	0.002	≤0.0075	0.025	$1.2^{+0.5}_{-0.9}$	0.44	2.3 ± 0.2
7→0	1904.2	$\frac{5}{2_3}^- \to \frac{3}{2_1}^-$	0.04	1.0 ± 0.2	2×10^{-4}	$(4.6^{+0.6}_{-0.7}) \times 10^{-3}$	0.62	$-(0.69^{+0.09}_{-0.006})$	2.1	36.3 ± 1.9
7→1	(1429.2)	$\frac{5}{2_3}^- \to \frac{1}{2_1}^-$	8.0						(27.1)	

TABLE VI *(Continued)*

Transition	E_γ [a] (keV)	$J^\pi_i \to J^\pi_f$	$B(E2)$ (W.u.) Theory [b]	$B(E2)$ (W.u.) Experiment [c]	$B(M1)$ (W.u.) Theory [b]	$B(M1)$ (W.u.) Experiment [c]	$\delta(E2/M1)$ Theory [b]	$\delta(E2/M1)$ Experiment [c]	Branching ratios (%) Theory [d]	Branching ratios (%) Experiment [e]
7→2	934.1	$\frac{5}{2}^-_3 \to \frac{5}{2}^-_1$	0.3	4.0 ± 1.2	0.086	0.061 ± 0.007	0.04	0.18 ± 0.03	75.8	41.6 ± 1.3
7→3	593.5	$\frac{5}{2}^-_3 \to \frac{7}{2}^-_1$		$3.8^{+2.0}_{-2.2}$		0.13 ± 0.02		$0.076^{+0.020}_{-0.022}$		22.1 ± 1.0
8→0	1932.5	$\frac{3}{2}^-_3 \to \frac{3}{2}^-_1$	0.007	$0.72^{+0.63}_{-0.35}$ or $8.7^{+1.6}_{-1.3}$	0.003	0.022 ± 0.003 or $(5.9^{+1.7}_{-3.0}) \times 10^{-3}$	0.07	$-(0.26^{+0.12}_{-0.08})$ or $-(1.82^{+0.54}_{-0.29})$	21.3	67.1 ± 4.3
8→1	1457.8	$\frac{3}{2}^-_3 \to \frac{1}{2}^-_1$	10.8	16 ± 2 or $0.67^{+0.46}_{-0.51}$	0.012	$(2.1 \pm 0.8) \times 10^{-3}$ or 0.020 ± 0.003	1.0	3.0 ± 0.8 or $-(0.20^{+0.07}_{-0.10})$	55.6	25.3 ± 1.7
8→2	962.5	$\frac{3}{2}^-_3 \to \frac{5}{2}^-_1$	0.80		0.026		0.12		23.1	7.6 ± 1.1
8→3	(622.1)	$\frac{3}{2}^-_3 \to \frac{7}{2}^-_1$	3.2						(0.2)	
8→4	(538.4)	$\frac{3}{2}^-_3 \to \frac{5}{2}^-_2$	4.5		0.22		0.056		(33.8)	
8→5	(272.3)	$\frac{3}{2}^-_3 \to \frac{3}{2}^-_2$	0.06		0.28		~0		(5.6)	
9→0	1942.4	$\frac{7}{2}^-_3 \to \frac{3}{2}^-_1$		$0.12^{+0.06}_{-0.05}$						10.4 ± 0.6
9→2	972.4	$\frac{7}{2}^-_3 \to \frac{5}{2}^-_1$								60 ± 4
9→3	631.9	$\frac{7}{2}^-_3 \to \frac{7}{2}^-_1$	1.0	$3.0^{+3.3}_{-2.6}$	0.48	0.013 ± 0.007	0.02	0.23 ± 0.07	18.4	19.2 ± 0.5
9→4	548.0	$\frac{7}{2}^-_3 \to \frac{5}{2}^-_2$	3.9		0.053		0.11		1.3	0.5 ± 0.1
9→5	(282.2)	$\frac{7}{2}^-_3 \to \frac{3}{2}^-_2$	2.4		0.014		0.2		(0.05)	
9→6	209.6	$\frac{7}{2}^-_3 \to \frac{7}{2}^-_2$		≤ 51		$0.19^{+0.10}_{-0.09}$		0.030 ± 0.052		9.9 ± 0.2
10→0	2088.7	$\frac{1}{2}^-_2 \to \frac{3}{2}^-_1$	5.9		0.002		2.6		53	68 ± 7

TABLE VI *(Continued)*

Transition	E_γ [a] (keV)	$J_i^\pi \to J_f^\pi$	$B(E2)$ (W.u.) Theory [b]	$B(E2)$ (W.u.) Experiment [c]	$B(M1)$ (W.u.) Theory [b]	$B(M1)$ (W.u.) Experiment [c]	$\delta(E2/M1)$ Theory [b]	$\delta(E2/M1)$ Experiment [c]	Branching ratios (%) Theory [d]	Branching ratios (%) Experiment [e]
10→1	1613.7	$\frac{1^-}{2_2} \to \frac{1^-}{2_1}$			0.03	0.043 ± 0.006			47.8	32 ± 3
10→2	(1118.7)	$\frac{1^-}{2_2} \to \frac{5^-}{2_1}$	0.03						(0.01)	

[a] Transitions indicated in parentheses have not been observed experimentally but transition rates have been calculated by Castel *et al.* (Ref. 1).
[b] From Castel *et al.* (Ref. 1).
[c] From this work as reported in Table V.
[d] These branching ratios have been calculated using the $B(E2)$ and $B(M1)$ values from columns 4 and 6 using the present experimental values for the transition energies as given in column 2. The theoretical branching ratios have been normalized to the sum of the experimental relative intensities for which common values exist. The values in parentheses are theoretical branching ratios for transitions that were not observed in the present work.
[e] From this work as reported in Table I.

tion is observed. It is also apparent that each of the $\frac{9}{2}^-$ states exhibits at least one strong $E2$ transition to levels below.

B. Comparison With Theory

As it was mentioned in the Introduction, of the three theoretical calculations[1-3] the one by Castel *et al.*[1] reported the most extensive results on the decay properties of the first 10 states in ^{61}Cu. In this calculation Castel *et al.*[1] included pairing effects and anharmonic effects in the coupling of the core with the $f_{7/2}$, $f_{5/2}$, $p_{3/2}$, and $p_{1/2}$ proton orbitals and have allowed only one adjustable parameter, the strength of the core-particle quadrupole interaction. The order of levels predicted by the calculation[1] reproduces the experimental order for the first five states as shown in Fig. 3 of Ref. 1. The second $\frac{1}{2}^-$ state, however, is predicted at 1.69 MeV which is low compared to 2.0889 MeV from experiment.

In Table VI we compare with experiment the values for $B(E2)$, $B(M1)$, $\delta(E2/M1)$, and branching

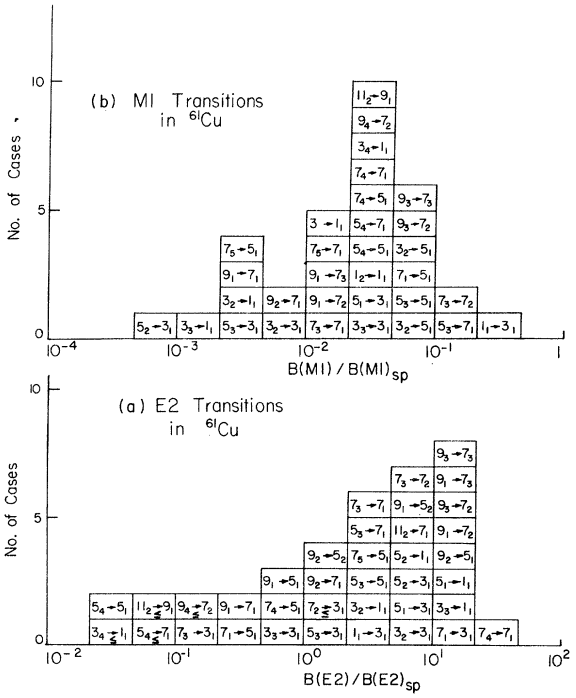

FIG. 10. Histograms representing the frequency distribution of the $B(E2)$ and $B(M1)$ values in W.u. for transitions in ^{61}Cu as determined in this work. The numbers in the boxes abbreviate the spin sequences (e.g. $7_5 \to 5_1$ abbreviates $\frac{7}{2}_5^- \to \frac{5}{2}_1^-$). In the case of levels with $J^\pi = \frac{3}{2}^-$ the values corresponding to one of the possible $\delta(E2/M1)$ which gives agreement with the results of Castel *et al.* (see Ref. 1) is included in the compilation. Upper limits are shown only if they correspond to the lower half of the frequency distribution.

fractions of Castel *et al.*[1] for the transitions from the first 10 levels in ^{61}Cu. The first three columns in Table VI give the transition numbers, the transition energy, and the spin sequence for each transition. Columns 4 and 6 in Table VI give the theoretical values for $B(E2)$ and $B(M1)$ in Weisskopf units from Ref. 1, while columns 5 and 7 give the corresponding experimental values from this work. The $\delta(E2/M1)$ values and branching ratios labelled theory in columns 8 and 10 were recalculated from the theoretical $B(E2)$ and $B(M1)$ values using the experimental transition energies. The theoretical branching ratios were normalized to the total intensity of the experimental values for the transitions for which both experimental and theoretical values are available. The transitions in parentheses in columns 2 and 10 have not been observed experimentally.

The comparison between experiment and theory for the $B(E2)$ values shows a good general agreement. For two transitions from the 1904.1-keV level, namely, to the ground and second excited state the theoretical $B(E2)$ values are lower by at least a factor of 10.

The comparison, on the other hand, of the theoretical and experimental $B(M1)$ values shows a less satisfactory agreement. There are three cases, namely, the transitions $2\rightarrow 0$, $7\rightarrow 0$, and $8\rightarrow 0$ with spin sequences $\frac{5}{2}^-_1\rightarrow\frac{3}{2}^-_1$, $\frac{5}{2}^-_3\rightarrow\frac{3}{2}^-_1$, and $\frac{3}{2}^-_3\rightarrow\frac{3}{2}^-_2$, respectively, for which the predicted rates are lower by a factor of ~10. There are three cases, namely, the transitions $4\rightarrow 0$, $6\rightarrow 2$, and $9\rightarrow 3$ with sequences $\frac{5}{2}^-_2\rightarrow\frac{3}{2}^-_1$, $\frac{7}{2}^-_2\rightarrow\frac{5}{2}^-_1$, and $\frac{7}{2}^-_3\rightarrow\frac{7}{2}^-_1$, respectively, for which the theoretical $B(M1)$ is higher by a factor of ~10. Finally, for 10 cases agreement between experimental and theoretical $B(M1)$ values with a factor of ~2 is observed.

In comparing the experimental and theoretical $\delta(E2/M1)$ values we notice that there are 5 cases out of the 14, for which comparison is possible, that are in agreement within experimental error. For the remaining nine cases the disagreement is larger than a factor of ~3 and well outside experimental error. In four cases ($4\rightarrow 0$, $6\rightarrow 0$, $8\rightarrow 1$, and $9\rightarrow 3$) the theoretical $\delta(E2/M1)$ is lower than experiment and the corresponding theoretical $B(M1)$ values are larger by a factor of ~10. In one case for the $2\rightarrow 0$ transition the theoretical $\delta(E2/M1)$ value is too high and this is correlated with a theoretical $B(M1)$ that is too small by ~10.

The comparison of the experimental and theoretical branching ratios shows moderate agreement for the levels Nos. 1, 2, 3, 4, 5, 9, and 10. Large discrepancies are observed for the levels 6, 7, and 8.

The present comparison of the experimental transition rates with the calculations of Castel *et al.*[1] shows that the particle-core model which properly accounts for the so-called anharmonic effects in the deformation of the core and includes pairing effects adequately describes the nuclear structure of ^{61}Cu and presumably that of ^{63}Cu and ^{65}Cu for which fewer transition rates are available. The present results of transition rates could further test the validity of the coupling scheme[1] by comparison with theory of the transition rates for the decay of three $\frac{9}{2}^-$ and two $\frac{11}{2}^-$ states in ^{61}Cu for which we obtained experimental values.

The authors express their thanks to R. Braga for carefully performing the statistical-model calculations of the singles angular distributions. The continued cooperation of the staff of the Washington University cyclotron is appreciated.

APPENDIX

The reduced transition probabilities $B(\sigma L)$ for transitions of multipole character (σL) were determined from experimental quantities with the aid of the expression:

$$B(\sigma L)=C(\sigma L)\frac{1}{\tau_{1\text{evel}}}f\,\Delta\frac{1}{1+\alpha_T}\frac{1}{E_\gamma^{2L+1}}\ (\text{units of } e^2\text{fm}^{2L}),$$

where

$$C(\sigma L)=\frac{L[(2L+1)!!]^2}{8\pi(L+1)}\frac{\hbar^{2(L+1)}c^{2L+1}}{e^2}$$

$$(\text{units of } e^2\text{fm}^{2L}\,\text{MeV}^{2L+1}\text{sec}),$$

$\tau_{1\text{evel}}$ is the mean lifetime of the level in sec, f is the branching fraction, $\Delta=1/(1+\delta^2)$ for the lower multipole $M1$, $E1$, etc. or $\Delta=\delta^2/(1+\delta^2)$ for the higher multipole of the mixed transition $E2$, $M2$, etc., α_T is the total conversion coefficient, and E_γ is the transition energy in MeV. For the above units $C(E2)=8.161\times10^{-10}$ and $C(M1)=6.2881\times10^{-16}$.

Values for α_T were estimated from the tables of Hager and Seltzer[29] for transitions below 500 keV.

The single-proton estimates were evaluated via the expressions[30]

$$B_{\text{sp}}(EL)\downarrow=\frac{1}{4\pi}\left(\frac{3}{3+L}\right)^2 1.2^{2L}A^{2L/3}\ (e^2\text{fm}^{2L})$$

and

$$B_{\text{sp}}(ML)\downarrow=\frac{0.1106}{\pi}\left(\frac{3}{3+L}\right)^2 1.2^{2L-2}A^{(2L-2)/3}\,(e^2\text{fm}^{2L}).$$

The tabulated transition strengths in columns 5 and 7 of Table V labeled (W.u.) are the ratios B/B_{sp}.

*Work supported in part by the U. S. Atomic Energy Commission under Contracts No. AT(11-1)-1530 and No. AT(11-1)-1760.

†Work supported in part by the National Science Foundation.

[1]B. Castel, I. P. Johnstone, B. P. Singh, and K. W. C. Stewart, Can. J. Phys. **50**, 1630 (1972).

[2]D. Larner, Phys. Rev. C **2**, 522 (1970).

[3]J. M. Gomez, Nucl. Phys. **A173**, 537 (1971).

[4]E. J. Hoffman and D. G. Sarantites, Nucl. Phys. **A157**, 584 (1970).

[5]E. J. Hoffman and D. G. Sarantites, Phys. Rev. **177**, 1647 (1969).

[6]G. H. Dulfer, B. O. ten Brink, T. J. Ketel, A. W. B. Kalshoven, and H. Verheul, Z. Phys. **251**, 416 (1972).

[7]B. Heusch, B. Cujec, R. Dayras, J. N. Mo, and I. M. Szöghy, Nucl. Phys. **A169**, 145 (1971).

[8]E. J. Hoffman, D. G. Sarantites, and N.-H. Lu, Nucl. Phys. **A173**, 146 (1971).

[9]E. J. Hoffman and D. G. Sarantites, Nucl. Phys. **A173**, 177 (1971).

[10]J. H. Barker and D. G. Sarantites, to be published.

[11]E. J. Hoffman, D. M. Van Patter, D. G. Sarantites, and J. H. Barker, Nucl. Instrum. Methods **109**, 3 (1973).

[12]B. Heusch, B. Cujec, and R. Dayras, Nucl. Phys. **A172**, 395 (1971).

[13]D. G. Sarantites and W. G. Winn, Nucl. Phys. **A149**, 647 (1970).

[14]F. Rauch, D. M. Van Patter, P. F. Hinrichsen, Nucl. Phys. **A124**, 145 (1969).

[15]M. E. Phelps, D. G. Sarantites, and W. G. Winn, Nucl. Phys. **A149**, 647 (1970).

[16]A. E. Blaugrund, Nucl. Phys. **88**, 501 (1966).

[17]L. Lindhard, M. Scharff, and H. E. Schiott, K. Dan. Vidensk. Selsk. Mat.-Fys. Medd. **33** (14)(1963).

[18]J. C. Ritter and R. E. Larson, Nucl. Phys. **A127**, 399 (1969).

[19]W. G. Winn and D. G. Sarantites, Nucl. Instrum. Methods **66**, 61 (1968); Nucl. Instrum. Methods **82**, 230 (1970).

[20]D. C. Camp and A. V. Van Lehn, Nucl. Instrum. Methods **76**, 192 (1969).

[21]H. J. Rose and D. M. Brink, Rev. Mod. Phys. **39**, 306 (1967).

[22]W. Hauser and H. Feshbach, Phys. Rev. **87**, 366 (1952).

[23]E. Sheldon and R. M. Strang, Comput. Phys. Commun. **1**, 35 (1969).

[24]E. Sheldon and D. M. Van Patter, Rev. Mod. Phys. **38**, 143 (1966).

[25]A. S. Mani, M. A. Melkanoff, and I. Iori, CEA Report No. CEA 2379, 1963 (unpublished).

[26]C. B. Fulmer, J. Benveniste, and A. C. Mitchell, Phys. Rev. **165**, 1218 (1968).

[27]D. Cline and P. M. S. Lesser, Nucl. Instrum. Methods **82**, 291 (1970).

[28]D. J. Pullen and B. Rosner, Phys. Rev. **170**, 1034 (1968).

[29]R. S. Hager and E. C. Seltzer, Nucl. Data **A4**, 1 (1968).

[30]S. J. Skorka, J. Hertel, and T. W. Retz-Schmidt, Nucl. Data **A2**, 347 (1966).